The Plant Cell, Vol. 31: 2187–2205, September 2019, www.plantcell.org © 2019 ASPB.

LEUNIG_HOMOLOG Mediates MYC2-Dependent Transcriptional Activation in Cooperation with the Coactivators HAC1 and MED25[OPEN]

Yanrong You,[a,b,1] Qingzhe Zhai,[a,1,2] Chunpeng An,[a,b] and Chuanyou Li[a,b,2]

[a] State Key Laboratory of Plant Genomics, National Center for Plant Gene Research (Beijing), Institute of Genetics and Developmental Biology, Chinese Academy of Sciences, Beijing 100101, China
[b] University of Chinese Academy of Sciences, Beijing, 100049, China

ORCID IDs: 0000-0002-6175-7993 (Y.Y.); 0000-0001-7423-4238 (Q.Z.); 0000-0003-1216-0047 (C.A.); 0000-0003-0202-3890 (C.L.)

Groucho/Thymidine uptake 1 (Gro/Tup1) family proteins are evolutionarily conserved transcriptional coregulators in eukaryotic cells. Despite their prominent function in transcriptional repression, little is known about their role in transcriptional activation and the underlying mechanism. Here, we report that the plant Gro/Tup1 family protein LEUNIG_HOMOLOG (LUH) activates MYELOCYTOMATOSIS2 (MYC2)-directed transcription of *JAZ2* and *LOX2* via the Mediator complex coactivator and the histone acetyltransferase HAC1. We show that the Mediator subunit MED25 physically recruits LUH to MYC2 target promoters that then links MYC2 with HAC1-dependent acetylation of Lys-9 of histone H3 (H3K9ac) to activate *JAZ2* and *LOX2*. Moreover, LUH promotes hormone-dependent enhancement of protein interactions between MYC2 and its coactivators MED25 and HAC1. Our results demonstrate that LUH interacts with MED25 and HAC1 through its distinct domains, thus imposing a selective advantage by acting as a scaffold for MYC2 activation. Therefore, the function of LUH in regulating jasmonate signaling is distinct from the function of TOPLESS, another member of the Gro/Tup1 family that represses MYC2-dependent gene expression in the resting stage.

INTRODUCTION

Jasmonate (JA) is a lipid-derived plant hormone that plays vital roles in regulating plant defense responses against mechanical wounding, herbivore attack, and pathogen infection (Browse, 2009; Wasternack and Hause, 2013; Zhai et al., 2017b). MYELOCYTOMATOSIS2 (MYC2), a basic helix-loop-helix transcription factor, is a master regulator of JA signaling that differentially regulates diverse aspects of JA responses (Boter et al., 2004; Lorenzo et al., 2004; Dombrecht et al., 2007; Kazan and Manners, 2013; Zhai et al., 2013; Du et al., 2017). In the resting stage, a group of JASMONATE ZIM DOMAIN (JAZ) proteins physically bind and inhibit MYC2 and related MYC transcription factors (Chini et al., 2007; Thines et al., 2007; Sheard et al., 2010; Fernández-Calvo et al., 2011; Qi et al., 2015; Song et al., 2017). This JAZ-mediated inhibition of MYC transcription factors is partly achieved via the recruitment of the TOPLESS (TPL) class of the Groucho/Thymidine uptake 1 (Gro/Tup1) family of corepressors (Pauwels et al., 2010; Zhang et al., 2015). It is believed that TPL epigenetically represses MYC2-regulated gene expression through recruitment of repressive histone modification enzymes and other chromatin remodelers (Zhu et al., 2011; Zhang et al., 2017). In response to internal or external cues, jasmonoyl-isoleucine (JA-Ile), the receptor-active form of JA, is rapidly synthesized by JASMONATE RESISTANT1 (JAR1; Staswick and Tiryaki, 2004; Fonseca et al., 2009). The perception of JA-Ile involves the formation of a coreceptor complex consisting of JAZ, JA-Ile, and CORONATINE INSENSITIVE1 (COI1), which is the F-box subunit of a functional SCF-type E3 ubiquitin ligase (Xie et al., 1998; Sheard et al., 2010). The JA-Ile–mediated JAZ–COI1 interaction leads to proteasome-dependent degradation of JAZ repressors, which derepresses MYC2 (Yan et al., 2009; Sheard et al., 2010).

Despite these advances in our understanding of the mechanisms involved in transcriptional repression and hormone perception (Chini et al., 2007; Thines et al., 2007; Pauwels et al., 2010; Zhang et al., 2015), less studied are the molecular details of hormone-dependent activation of MYC2. The Mediator complex is an evolutionarily conserved multisubunit coactivator complex whose activity is essential for RNA polymerase II (Pol II)–dependent gene transcription in eukaryotic cells (Bäckström et al., 2007; Kornberg, 2007; Malik and Roeder, 2010; Soutourina et al., 2011; Fondell, 2013; Poss et al., 2013; Yin and Wang, 2014; Allen and Taatjes, 2015). We and others have previously demonstrated that the Arabidopsis (*Arabidopsis thaliana*) Mediator subunit MED25 plays multiple roles in JA-triggered activation of MYC2 (Çevik et al., 2012; Chen et al., 2012; An et al., 2017; Zhai et al., 2017a). First, MED25 physically and functionally interacts with MYC2, thereby playing a pivotal role in preinitiation complex assembly during MYC2-dependent transcription of JA-responsive genes (Chen et al., 2012). Second, MED25 physically recruits COI1 to MYC2 target promoters in the resting stage and facilitates COI1-dependent degradation of JAZ repressors in the presence of JA-Ile (An et al., 2017). Third, MED25 physically

[1] These authors contributed equally to this work.
[2] Address correspondence to cyli@genetics.ac.cn or qzzhai@genetics.ac.cn.
The author responsible for distribution of materials integral to the findings presented in this article in accordance with the policy described in the Instructions for Authors (www.plantcell.org) is: Chuanyou Li (cyli@genetics.ac.cn).
[OPEN]Articles can be viewed without a subscription.
www.plantcell.org/cgi/doi/10.1105/tpc.19.00115

IN A NUTSHELL

Background: Jasmonate (JA) is a lipid-derived plant hormone that regulates plant defense responses against mechanical wounding, herbivore attack, and pathogen infection. MYC2 is a master transcription factor that regulates diverse aspects of JA responses. At low JA levels, JASMONATE ZIM DOMAIN (JAZ) repressor proteins recruit the Groucho/Tup1 family corepressor TOPLESS (TPL) to inhibit MYC2-dependent activation of JA-responsive genes. Following hormone-dependent degradation of JAZ repressors, MYC2 is released. The Mediator complex is an evolutionarily conserved multisubunit coactivator complex whose activity is essential for RNA polymerase II (Pol II)-dependent gene transcription in eukaryotic cells. Mediator subunit MED25 interacts directly with MYC2 and is involved in the assembly of a MYC2-MED25 functional transcription complex (MMC) during hormone-triggered activation of MYC2..

Questions: Are there any new components of this MMC that help MED25 to activate MYC2's transcriptional activity upon hormone perception? What are the molecular mechanisms of hormone-dependent activation of MYC2?

Findings: In contrast to TPL, which represses MYC2 in the resting stage, we found that two other Groucho/Tup1 family corepressors, LEUNIG (LUG) and LEUNIG_HOMOLOG (LUH), are components of the MMC, and they redundantly activate MYC2 upon hormone elicitation. LUH activates MYC2-directed transcription of JA-responsive genes via the Mediator complex coactivator and the histone acetyltransferase HAC1. MED25 directly recruits LUH to MYC2 target promoters, and then LUH links MYC2 with HAC1-dependent histone H3K9 acetylation to activate JA-responsive genes. We also found that LUH acts as a scaffold to coordinate the coactivators MED25 and HAC1 during JA-triggered activation of MYC2. Considering the role of TPL, our study demonstrates that different members of the plant Groucho/Tup1 family play antagonistic roles in regulating the same signaling pathway via distinct mechanisms.

Next steps: One interesting direction for future exploration is to identify the epigenetic partners of LUG and to elucidate their mechanisms of action during the activation of MYC2. Furthermore, our finding that LUH activates JA signaling can be exploited for improving the resistance of crop plants.

and functionally interacts with HISTONE ACETYLTRANSFERASE OF THE CBP FAMILY1 (HAC1), which selectively regulates hormone-induced acetylation of Lys-9 of histone H3 (H3K9ac) of MYC2 target promoters (An et al., 2017). Together, these studies led us to a hypothesis that MED25 is involved in the assembly of a MYC2-MED25 functional transcription complex (MMC), which acts as an integrative hub to coordinate the actions of multiple regulators during hormone-triggered activation of MYC2 (An et al., 2017).

Using an unbiased proteomic analysis of MED25-associated proteins in Arabidopsis, we established LEUNIG (LUG) and LEUNIG_HOMOLOG (LUH), two highly homologous members of the Gro/Tup1 family of transcriptional corepressors (Liu and Meyerowitz, 1995; Conner and Liu, 2000; Liu and Karmarkar, 2008; Sitaraman et al., 2008), as additional components of the MMC. In contrast to TPL, which represses MYC2 in the resting stage, LUH and LUG redundantly activate MYC2 upon hormone elicitation.

Here, we examine the mechanistic function of LUH in activating MYC2-regulated transcription of *JAZ2* and *LOX2*. We show that LUH is recruited to MYC2 target promoters via its physical interaction with MED25. Subsequently, LUH links MYC2 with HAC1 to activate MYC2 targets via H3K9ac. We demonstrate that LUH acts as a scaffold to coordinate the coactivators MED25 and HAC1 during JA-triggered activation of MYC2.

RESULTS

LUH Interacts with the Coactivator MED25 through Its Q-Rich Domain

MED25 acts as an integrator to coordinate MYC2-regulated transcriptional reprogramming during JA signaling (Çevik et al., 2012; Chen et al., 2012; An et al., 2017). In an attempt to identify additional components of the MMC, we analyzed total protein extracts prepared from *MED25-myc* transgenic plants (Chen et al., 2012) by affinity purification using anti-myc agarose beads, followed by mass spectrometric analysis. A large number of Mediator subunits were identified in our analysis, including MED5a, MED5b, MED6, MED8, MED10b, MED12, MED13, MED14, MED15, MED16, MED17, MED23, MED27, and MED35 (Supplemental Table 1), thus validating our approach. Our analysis also identified five transcriptional coregulators (Supplemental Table 1). We focused our analysis on LUH and LUG, the two most highly related members of the Gro/Tup family of transcriptional corepressors in Arabidopsis.

To confirm the interaction of LUH and LUG with MED25, we performed yeast two-hybrid (Y2H) assays using fusions of full-length LUH or LUG with the GAL4 DNA activation domain (AD) and full-length MED25 with the GAL4 DNA binding domain (BD). Results showed that both LUH and LUG interacted with MED25 in yeast (*Saccharomyces cerevisiae*; Figure 1A). The Y2H-based domain mapping assays indicated that the Gln-rich domain of LUH (Q-rich, LUH^{82-372}; Chen and Courey, 2000) and the middle domain (MD) of MED25, together with the activator-interacting domain (ACID) of MED25 (Chen et al., 2012), are involved in the LUH–MED25 interaction (Supplemental Figure 1). By contrast, TPL, which lacks the Q-rich domain, did not show interaction with MED25 in the Y2H assays (Figure 1A; Supplemental Figure 1A).

To confirm the physical interaction between MED25 and LUH, we performed in vitro pull-down experiments using purified maltose binding protein (MBP)–tagged LUH (MBP-LUH) and the MED25 protein fragment containing the MD and ACID domains tagged with glutathione S-transferase (GST-$MED25^{MA}$). The GST-$MED25^{MA}$ recombinant fusion protein, but not GST, was able to

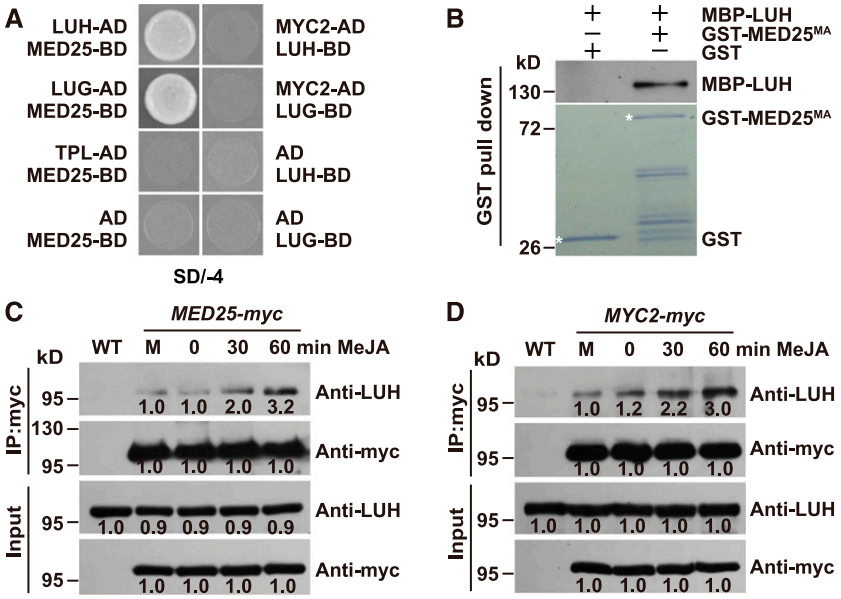

Figure 1. MED25 Interacts with LUH and LUG, but Not with TPL.

(A) Y2H assays examining interactions between the GAL4 DNA AD fusions of LUH, LUG, TPL, and MYC2, and GAL4 DNA BD fusions of MED25, LUH, and LUG. The transformed yeast cells were plated on SD medium lacking His, Ade, Leu, and Trp (SD/-4). The empty AD vector was used as a negative control.
(B) In vitro pull-down assays to verify the interaction between LUH and MED25. Purified MBP-LUH protein was incubated with GST or GST-MED25^{MA} (MD and ACID domains) for the GST pull-down assay and detected by immunoblotting using an anti-MBP antibody (top). The positions of purified GST and GST-MED25^{MA} proteins separated by SDS-PAGE are marked with asterisks on the Coomassie blue–stained gel (bottom).
(C) and **(D)** Co-IP assays to verify in vivo interactions between LUH and MED25 using 10-d-old *MED25-myc* seedlings **(C)** and between LUH and MYC2 using 10-d-old *MYC2-myc* seedlings **(D)**. Seedlings were treated with 0.1% (v/v) ethanol for 60 min (mock, M) or 100 μM MeJA for the indicated times. The wild-type (WT) seedlings were used as negative controls. Protein from each sample was immunoprecipitated using an anti-myc antibody and immunoblotted using an anti-LUH antibody. Bands were quantified using ImageJ software, and levels relative to the mock control are shown under each band. All experiments in **(A)** to **(D)** were repeated at least three times with similar results. IP, immunoprecipitation.

pull down LUH (Figure 1B), indicating that LUH interacts with MED25 in vitro.

To determine whether LUH interacts with MED25 in planta, we performed coimmunoprecipitation (Co-IP) experiments using our previously described *MED25-myc* plants overexpressing the *MED25* coding sequence fused with *myc* (Chen et al., 2012) and an anti-LUH antibody. As shown in Figure 1C, MED25 coimmunoprecipitated with endogenous LUH when using protein extracts prepared from *MED25-myc* seedlings, but not when using those prepared from the wild-type seedlings, indicating that LUH interacts with MED25 in vivo. Notably, the ability of MED25-myc to coimmunoprecipitate LUH was markedly increased following treatment with the methyl ester of JA (MeJA; Figure 1C), suggesting that the LUH–MED25 interaction was enhanced by hormone elicitation.

Considering that MED25 forms a transcriptional activation complex with MYC2 through a physical interaction (Chen et al., 2012; An et al., 2017), we investigated whether LUH and LUG interacted with MYC2 using Y2H assays. Using fusions of full-length LUH and LUG with the GAL4 BD and full-length MYC2 with the GAL4 AD, we found that neither LUH nor LUG interacted with MYC2 (Figure 1A). We then performed Co-IP experiments using our previously described *MYC2-myc* plants overexpressing the *MYC2* coding sequence fused with *myc* (Chen et al., 2011) and an anti-LUH antibody. We found that MYC2-myc coimmunoprecipitated with endogenous LUH (Figure 1D). Moreover, the ability of MYC2-myc to pull down endogenous LUH was substantially increased following MeJA treatment (Figure 1D). These results indicate that LUH associates with MYC2 in vivo, and the LUH–MYC2 association is enhanced by hormone treatment.

LUH Positively Regulates MYC2-Dependent Transcription of JA-Responsive Genes

To elucidate the biological significance of LUH–MED25 interaction, we obtained two T-DNA insertion mutant lines, *luh-3* (Sitaraman et al., 2008) and *luh-4* (Stahle et al., 2009), from the Arabidopsis Biological Resource Center (Supplemental Figure 2A). These lines showed a reduction in the level of *LUH* gene expression and LUH protein accumulation (Supplemental Figures 2B and 2C). We compared JA-responsive gene expression in the wild-type plants versus the T-DNA insertion *luh* mutants. The MeJA-induced expression of *VEGETATIVE STORAGE PROTEIN2* (*VSP2*), a marker of the JA-regulated wounding response (Berger et al., 1995), was significantly reduced in *luh* mutants compared with the wild type (Figure 2A). Similarly, the MeJA-induced expression of the plant defense gene *PDF1.2*, a marker of JA-regulated pathogen response (Penninckx et al., 1996), was significantly reduced in *luh* mutants compared with the wild type (Figure 2A). Unsurprisingly, the MeJA-induced expression of *JAZ2* (Figueroa and Browse, 2012) and *LIPOXYGENASE2* (*LOX2*; Bell

et al., 1995; Hou et al., 2010), which are direct transcriptional targets of MYC2, was also reduced in *luh* mutants compared with the wild type (Figure 2A). These results indicate that LUH positively regulates MYC2-mediated transcription of JA-responsive genes.

We then performed RNA sequencing (RNA-seq) experiments to compare the transcriptome profiles between the untreated wild-type and *luh-4* seedlings and similar seedlings treated with MeJA. We treated the 10-d-old wild-type and *luh-4* seedlings with 100 μM MeJA for 1, 6, or 24 h. The untreated wild-type and *luh-4* seedlings were used as controls. Seedlings from three biological replicates were collected for RNA extraction and sequencing. Quality assessment of the RNA-seq data is shown in Supplemental Figure 3A. We identified 3642 genes that were

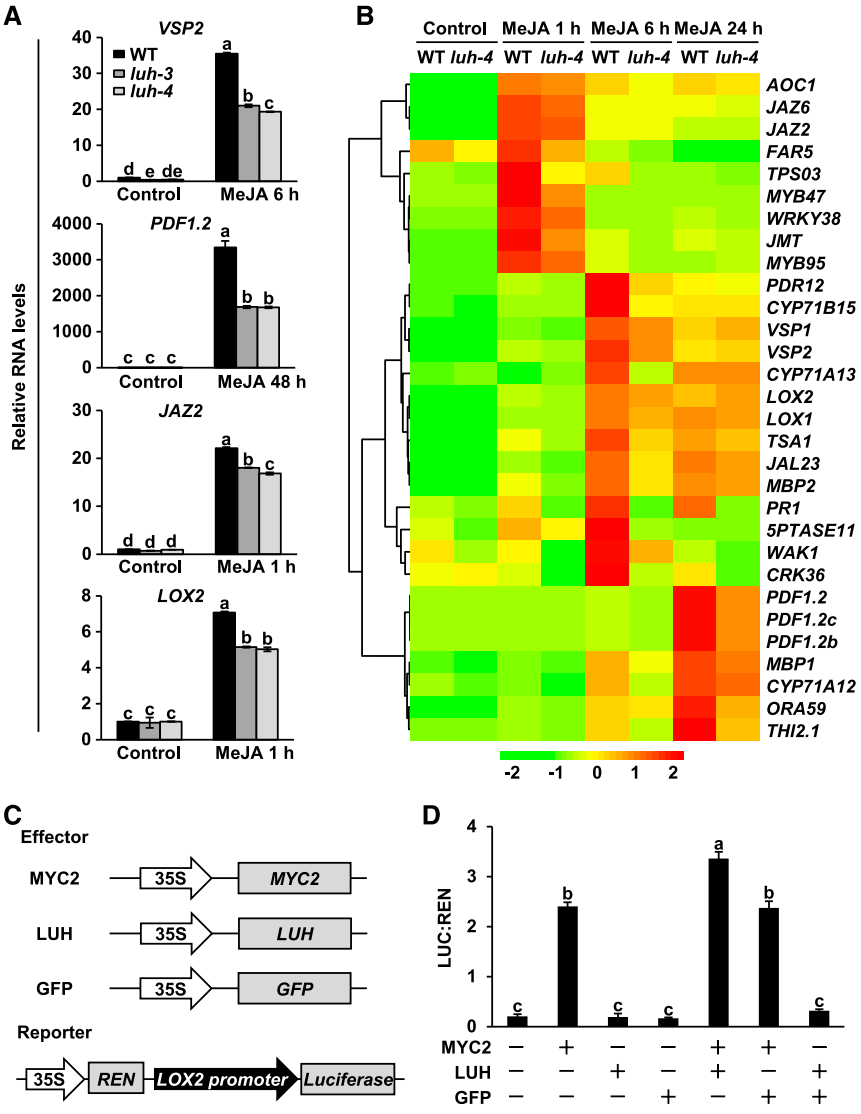

Figure 2. LUH Plays a Positive Role in MYC2-Regulated Expression of JA-Responsive Genes.

(A) RT-qPCR analysis showing MeJA-induced expression of *VSP2*, *PDF1.2*, *JAZ2*, and *LOX2* in 10-d-old wild-type (WT), *luh-3*, and *luh-4* seedlings treated with or without 100 μM MeJA for the indicated times. *ACTIN7* was used as the internal standard. Data are presented as mean ± SD. Different letters indicate significant difference at $P < 0.05$ ($n = 3$, one-way analysis of variance [ANOVA]), Tukey post test, three independent experiments; Supplemental File).
(B) Expression of the selected MeJA-responsive genes in the wild-type (WT) and *luh-4* plants in the RNA-seq experiments. Ten-day-old WT and *luh-4* seedlings were treated with 100 μM MeJA for 1, 6, or 24 h. Untreated WT and *luh-4* seedlings were used as controls. Three biological replicates were performed. Colors on the scale bar indicate log fold change. Fold change of the average expression of each gene from three biological replicates is shown.
(C) Schematic diagram showing the constructs used in the transient expression assays of **(D)**. Arrows, promoter regions; shaded boxes, coding regions.
(D) Transient expression assays in Arabidopsis protoplasts showing that activation of the *LOX2* promoter by MYC2 is stimulated by LUH. The *ProLOX2:LUC* reporter was cotransformed with the indicated effector constructs. The LUC:REN ratio represents the *ProLOX2:LUC* activity relative to the internal control (*REN* driven by the 35S promoter). Data are presented as mean ± SD. Different letters indicate significant difference at $P < 0.05$ ($n = 3$, one-way ANOVA, Tukey post test, three independent experiments; Supplemental File).

upregulated by MeJA at any time point (1, 6, or 24 h) in the wild type (fold change > 1.5, false discovery rate [FDR]–adjusted P < 0.05). We also identified 654 genes whose expression was significantly reduced in *luh-4* compared with the wild type at any time point after MeJA treatment (fold change > 1.5, FDR-adjusted P < 0.05; Supplemental Figure 3B; Supplemental Data Set 1). Comparison of these two sets of genes led to the identification of 203 genes showing significantly reduced expression in MeJA-treated *luh-4* seedlings compared with MeJA-treated wild-type seedlings (fold change > 1.5, FDR adjusted P < 0.05; Supplemental Figure 3B; Supplemental Data Set 2). Thus, LUH is involved in the activation of a subset (i.e., 203 of 3642) of the MeJA-upregulated genes. These 203 genes were defined as LUH– and MeJA–co-upregulated genes. Gene ontology (GO) analysis indicated that these genes are enriched in pathways related to JA response, fungus defense response, and insect defense response (Supplemental Data Set 2). The top ten enriched biological processes are shown in Supplemental Figure 3D. Many well-characterized JA-inducible genes were identified as LUH– and MeJA–co-upregulated genes (Figure 2B; Supplemental Data Set 2). This list includes genes involved in JA metabolism, JA signaling, and JA-induced defense responses (Figure 2B).

In parallel, we identified 4045 genes that were downregulated by MeJA in the wild type (fold change > 1.5, FDR-adjusted P < 0.05). We also identified 252 genes whose expression was significantly higher in *luh-4* compared with the wild type at any time point after MeJA treatment (fold change > 1.5, FDR-adjusted P < 0.05; Supplemental Figure 3C; Supplemental Data Set 3). Comparison of these two sets of genes led to the identification of 108 genes that were less repressed in MeJA-treated *luh-4* seedlings compared with the MeJA-treated wild-type seedlings (fold change > 1.5, FDR-adjusted P < 0.05; Supplemental Figure 3C; Supplemental Data Set 4). Thus, LUH is involved in the repression of ~2.7% (i.e., 108 of 4045) of the MeJA-downregulated genes. These 108 genes were defined as LUH– and MeJA–co-downregulated genes. GO analysis indicated that this group of genes does not show significant enrichment in any biological processes (Supplemental Data Set 4).

The transcriptome analysis suggests that LUH positively regulates a statistically significant but relatively small proportion (203 of 3642) of MeJA-induced genes. This might be because LUG and LUH share redundant functions in positively regulating JA-responsive genes and that the stringent cutoffs we used to determine differential expression have excluded some legitimately regulated genes.

Next, we used a well-established dual-luciferase (LUC) reporter system (Hellens et al., 2005) to verify that LUH acts as a coactivator of MYC2. For this purpose, we cloned a 1745-bp *LOX2* promoter sequence into the dual-LUC reporter system to generate a *ProLOX2:LUC* reporter construct (Figure 2C). Coexpression of MYC2 with *ProLOX2:LUC* in Arabidopsis protoplasts led to significantly increased LUC activity (Figures 2C and 2D), suggesting that MYC2 activates the expression of *ProLOX2:LUC*. When LUH was coexpressed with MYC2 and the *ProLOX2:LUC* reporter, the MYC2-dependent activation of LUC activity was further enhanced (Figures 2C and 2D). In parallel control experiments, green fluorescent protein (GFP) showed a negligible effect on MYC2-dependent activation of LUC activity. Taken together, these results support that, in contrast to TPL, which acts as a corepressor of MYC2 (Pauwels et al., 2010; Zhang et al., 2015), LUH functions as a coactivator of MYC2 during JA signaling.

LUG and LUH Perform Redundant Functions in Regulating JA Signaling

In Co-IP experiments using *MED25-myc* plants (Chen et al., 2012) and an anti-LUG antibody, MED25-myc pulled down native LUG (Supplemental Figure 4A), demonstrating the association between LUG and MED25 in vivo. Taking into account the functional redundancy of LUG and LUH in regulating development (Sitaraman et al., 2008; Stahle et al., 2009), we hypothesized that these proteins may also share redundant functions in the activation of MYC2-dependent transcription of JA-responsive genes.

To test this hypothesis, we set out to identify a *luh lug* double mutant line from a cross between *luh-4* and the T-DNA insertion mutant *lug-444* (Stahle et al., 2009). Consistent with previous observations (Liu and Meyerowitz, 1995; Sitaraman et al., 2008; Stahle et al., 2009), the homozygous *lug-444* mutant is sterile and did not show obvious defects at the seedling stage (Supplemental Figure 4B), but it developed serrated rosette leaves after growing on the medium for more than 20 d (Supplemental Figure 4C). PCR-based genotyping together with phenotypic observations indicated that *luh-4 lug-444*/+ (homozygous for *luh-4* and heterozygous for *lug-444*) plants showed abnormal cotyledons (Supplemental Figure 4D). Close observation of the siliques of *luh-4 lug-444*/+ plants revealed that ~25% of the seeds were embryonic lethal (Supplemental Figure 4E). This confirmed that the *luh-4 lug-444* (homozygous for both *luh-4* and *lug-444*) mutant is embryonic lethal (Sitaraman et al., 2008; Stahle et al., 2009).

Hence, *luh-4 lug-444*/+ plants were used in the following experiments. We examined MeJA-induced expression of an array of JA-responsive genes in the wild-type, *luh-4*, *lug-444*, and *luh-4 lug-444*/+ plants and found that the MeJA-induced expression of *VSP2*, *PDF1.2*, *JAZ2*, and *LOX2* was significantly reduced in *lug-444* mutants compared with the wild type (Figure 3A), indicating that, like LUH, LUG also positively regulates MYC2-dependent transcription of JA-responsive genes. Moreover, the expression levels of *VSP2*, *PDF1.2*, *JAZ2*, and *LOX2* were significantly lower in *luh-4 lug-444*/+ plants than those in any of their parental lines after MeJA treatment (Figure 3A), revealing that LUG functions redundantly with LUH in activating MYC2-dependent transcription of JA-responsive genes.

Next, we examined the wild-type, *luh-4*, *lug-444*, and *luh-4 lug-444*/+ plants that were subjected to herbivorous insect attack. For these experiments, mature rosette leaves from 4-week-old plants were fed on by *Spodoptera exigua*, a globally significant agricultural pest with a broad host range (Howe and Jander, 2008). *S. exigua* larvae consumed more leaves and grew stronger when fed with *luh-4* and *lug-444* mutant leaves than did the larvae fed with the wild-type leaves (Figures 3B and 3C), suggesting that LUH and LUG positively regulate plant defense against insect attack. Moreover, *S. exigua* larvae fed with *luh-4 lug-444*/+ leaves consumed more tissues and grew stronger than those fed with single mutant leaves (Figures 3B and 3C), indicating that LUG acts

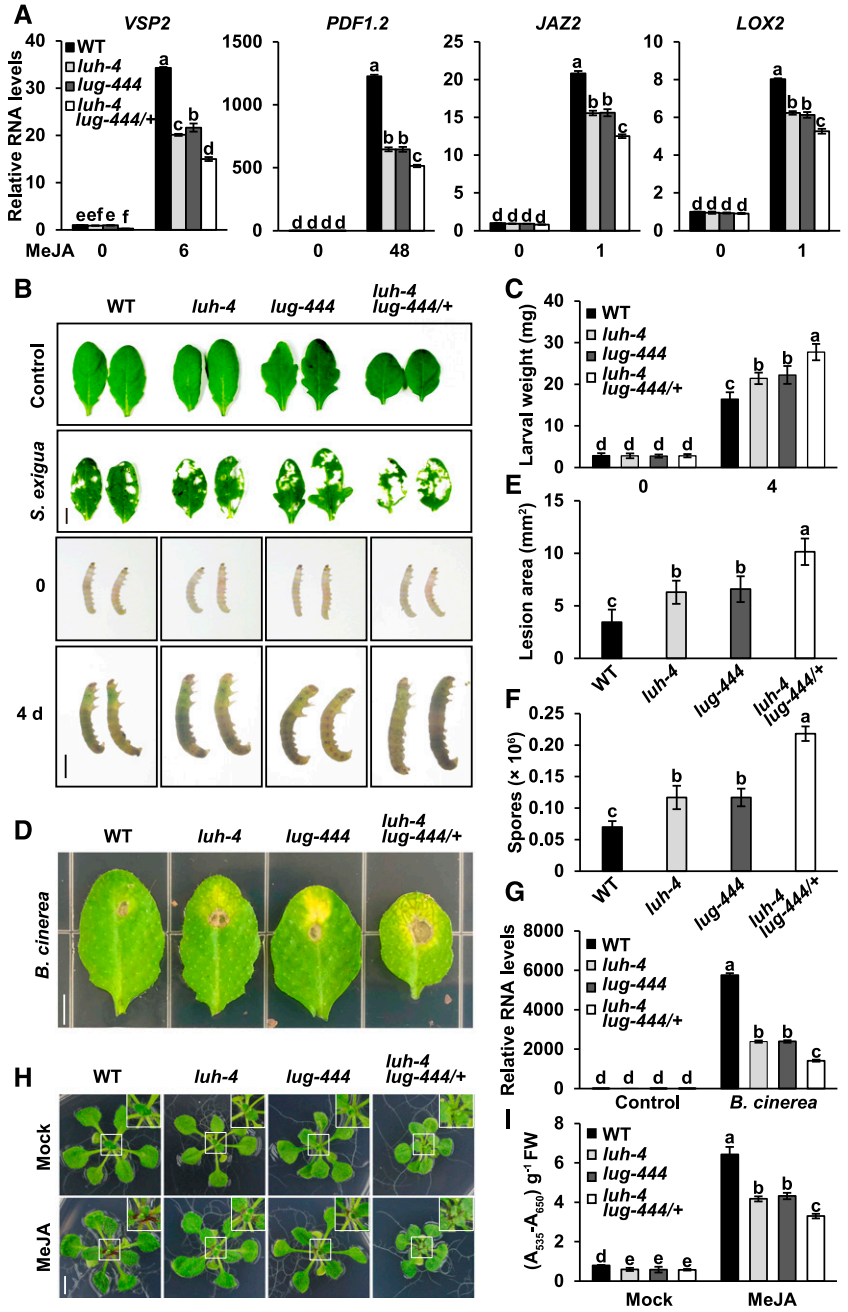

Figure 3. LUG Acts Redundantly with LUH in Positively Regulating Diverse Aspects of JA Responses.

(A) RT-qPCR analysis showing the expression of *VSP2*, *PDF1.2*, *JAZ2*, and *LOX2* in the 21-d-old wild-type (WT), *luh-4*, *lug-444*, and *luh-4 lug-444/+* seedlings treated with or without 100 μM MeJA for the indicated times (in hours). *ACTIN7* was used as the internal standard. Data are presented as mean ± SD. Different letters indicate significant difference at $P < 0.05$ ($n = 3$, one-way ANOVA, Tukey post test, three independent experiments; Supplemental File).

(B) Insect feeding assays. (Top) Representative rosette leaves of the 4-week-old wild-type (WT), *luh-4*, *lug-444*, and *luh-4 lug-444/+* plants without feeding (control) or with feeding by *S. exigua*. Bar = 5 mm. (Bottom) Representative third-instar *S. exigua* larvae before feeding (0) or 4 d after feeding (4 d) on rosette leaves of indicated plants. Bar = 5 mm.

(C) Average weight of each third-instar *S. exigua* larva before (0) or after feeding on rosette leaves of the 4-week-old wild-type (WT), *luh-4*, *lug-444*, and *luh-4 lug-444/+* plants for 4 d (4). Data are presented as mean ± SD. Different letters indicate significant difference at $P < 0.05$ ($n = 15$, one-way ANOVA, Tukey post test, three independent experiments; Supplemental File).

(D) and **(E)** Response of the wild-type (WT), *luh-4*, *lug-444*, and *luh-4 lug-444/+* plants to *B. cinerea* infection. Four-week-old plants were spotted with a 5-μL *B. cinerea* spore suspension (5×10^5 spores/mL) or with potato dextrose broth (control, Supplemental Figure 4F). Photographs of disease lesions **(D)** and

redundantly with LUH in regulating plant defense against insect attack.

To investigate the role of LUH and LUG in plant resistance against pathogen infection, we challenged the wild-type, *luh-4*, *lug-444*, and *luh-4 lug-444*/+ plants with the necrotrophic fungus *Botrytis cinerea*. *B. cinerea* infection led to significantly larger necrotic lesions and increased spore accumulation in *luh-4* and *lug-444* leaves than in the wild-type leaves (Figures 3D to 3F; Supplemental Figure 4F). In addition, the expression of the plant defense gene *PDF1.2* was significantly reduced in *B. cinerea*–infected *luh-4* and *lug-444* leaves compared with the wild type (Figure 3G), indicating that LUH and LUG positively regulate plant resistance to *B. cinerea*. Moreover, *B. cinerea*–induced necrotic lesions on the leaves of *luh-4 lug-444*/+ plants were significantly larger than those on the leaves of *luh-4* and *lug-444* plants (Figures 3D and 3E; Supplemental Figure 4F), and the fungal spore accumulation in *luh-4 lug-444*/+ leaves was significantly higher than that in *luh-4* or *lug-444* leaves (Figure 3F). Consistently, the expression of *PDF1.2* was significantly reduced in *B. cinerea*–infected *luh-4 lug-444*/+ leaves compared with that in *luh-4* and *lug-444* leaves (Figure 3G). These results demonstrate that LUH and LUG act redundantly in positively regulating plant resistance against *B. cinerea* infection.

In agreement with previous observations (Li et al., 2004; Qi et al., 2011), we found that exogenous application of MeJA to the wild-type seedlings led to anthocyanin accumulation (Figures 3H and 3I) and that this accumulation was significantly less in *luh-4* and *lug-444* plants compared with the wild type (Figures 3H and 3I). Notably, MeJA-induced anthocyanin accumulation was found to be significantly lower in *luh-4 lug-444*/+ plants compared with *luh-4* and *lug-444* plants (Figures 3H and 3I), although the basal levels of anthocyanin accumulation in *luh-4*, *lug-444*, and *luh-4 lug-444*/+ were slightly lower than in the wild type. These results indicate that LUH and LUG positively regulate anthocyanin accumulation and that they function redundantly in MeJA-induced anthocyanin accumulation.

In JA-induced root growth inhibition assays, we found that JA-induced root growth inhibition was similar among the wild type and *luh-4*, *lug-444* as well as *luh-4 lug-444*/+ mutants (Supplemental Figure 4G), suggesting that LUH and LUG have a minor, if any, effect on JA-induced root growth inhibition. Taken together, our results indicated that LUG and LUH perform redundant functions in regulating JA signaling.

MED25 Is Important for JA-Induced Recruitment of LUH to MYC2 Target Promoters

To measure the enrichment of LUH on the chromatin of the MYC2 targets *JAZ2* and *LOX2*, we performed chromatin immunoprecipitation-quantitative PCR (ChIP-qPCR) assays on transgenic plants expressing a 3′ translational fusion of LUH with the GFP reporter (LUH-GFP; Supplemental Figures 5A and 5B) using an anti-GFP antibody. Results of ChIP-qPCR analyses revealed that the level of LUH enrichment at the G-box and transcription start site (TSS) of *JAZ2* and *LOX2* was much higher than the level in either the upstream promoter region or the coding sequence of both genes (Figures 4A and 4B). This indicated that LUH is mainly enriched in the promoter regions (G-box and TSS) of MYC2 targets.

To determine whether JA signaling regulates the enrichment of LUH at the promoter region of MYC2 targets, we performed a time-course assay to examine MeJA-induced enrichment of LUH at the G-boxes of *JAZ2* and *LOX2*. The level of LUH enrichment peaked within 30 min of MeJA treatment and subsequently declined (Figures 4A and 4C), whereas the protein levels of LUH-GFP did not show obvious change upon MeJA treatment (Supplemental Figure 5C). Similarly, LUG-GFP was also enriched in the G-box regions of MYC2 targets, and the enrichment level increased after MeJA treatment (Supplemental Figures 6A and 6B), whereas the protein levels of LUG-GFP did not show an obvious change upon MeJA treatment (Supplemental Figure 6C). In parallel experiments, the MeJA-induced recruitment of LUH to the G-box regions of *JAZ2* and *LOX2* was substantially reduced in the *coi1-2* mutant (Figures 4A and 4D; Xu et al., 2002), even though that *COI1* mutation does not affect the protein level of LUH-GFP (Supplemental Figure 5D), suggesting that COI1-dependent JA signaling regulates the recruitment of LUH to MYC2 target promoters.

To further understand the mechanism of LUH recruitment to MYC2 target promoters, we examined whether the depletion of MYC2 or MED25 affected the enrichment levels of LUH at the

Figure 3. (continued).

lesion areas **(E)** are shown 3 d after inoculation. Bar = 5 mm. Data are presented as mean ± SD. Different letters indicate significant difference at $P < 0.05$ ($n = 15$, one-way ANOVA, Tukey post test, three independent experiments; Supplemental File).

(F) Growth of *B. cinerea* in the wild-type (WT), *luh-4*, *lug-444*, and *luh-4 lug-444*/+ plants. Four-week-old plants were spotted with a 5-μL *B. cinerea* spore suspension (5×10^5 spores/mL). Sixteen spotted leaves of each genotype were harvested 3 d after inoculation, and the numbers of spores were counted. The numbers of spores per leaf of each genotype are shown. Data are presented as mean ± SD. Different letters indicate significant difference at $P < 0.05$ ($n = 5$, one-way ANOVA, Tukey post test, three independent experiments; Supplemental File).

(G) *B. cinerea*–induced expression of plant defense genes *PDF1.2* in the wild-type (WT), *luh-4*, *lug-444*, and *luh-4 lug-444*/+ plants. Four-week-old plants were spotted with a 5-μL *B. cinerea* spore suspension (5×10^5 spores/mL). The spotted leaves were harvested 3 d after inoculation for RNA extraction and RT-qPCR analysis. *ACTIN7* was used as the internal standard. Data are presented as mean ± SD. Different letters indicate significant difference at $P < 0.05$ ($n = 3$, one-way ANOVA, Tukey post test, three independent experiments; Supplemental File).

(H) Representative images of the 21-d-old wild-type (WT), *luh-4*, *lug-444*, and *luh-4 lug-444*/+ plants grown on half strength MS medium treated with or without 100 μM MeJA for 48 h. Bar = 5 mm.

(I) Anthocyanin contents of the 21-d-old seedlings in the wild-type (WT), *luh-4*, *lug-444*, and *luh-4 lug-444*/+ plants treated with or without 100 μM MeJA for 48 h. Data are presented as mean ± SD. Different letters indicate significant difference at $P < 0.05$ ($n = 3$, one-way ANOVA, Tukey post test, three independent experiments; Supplemental File). FW, fresh weight.

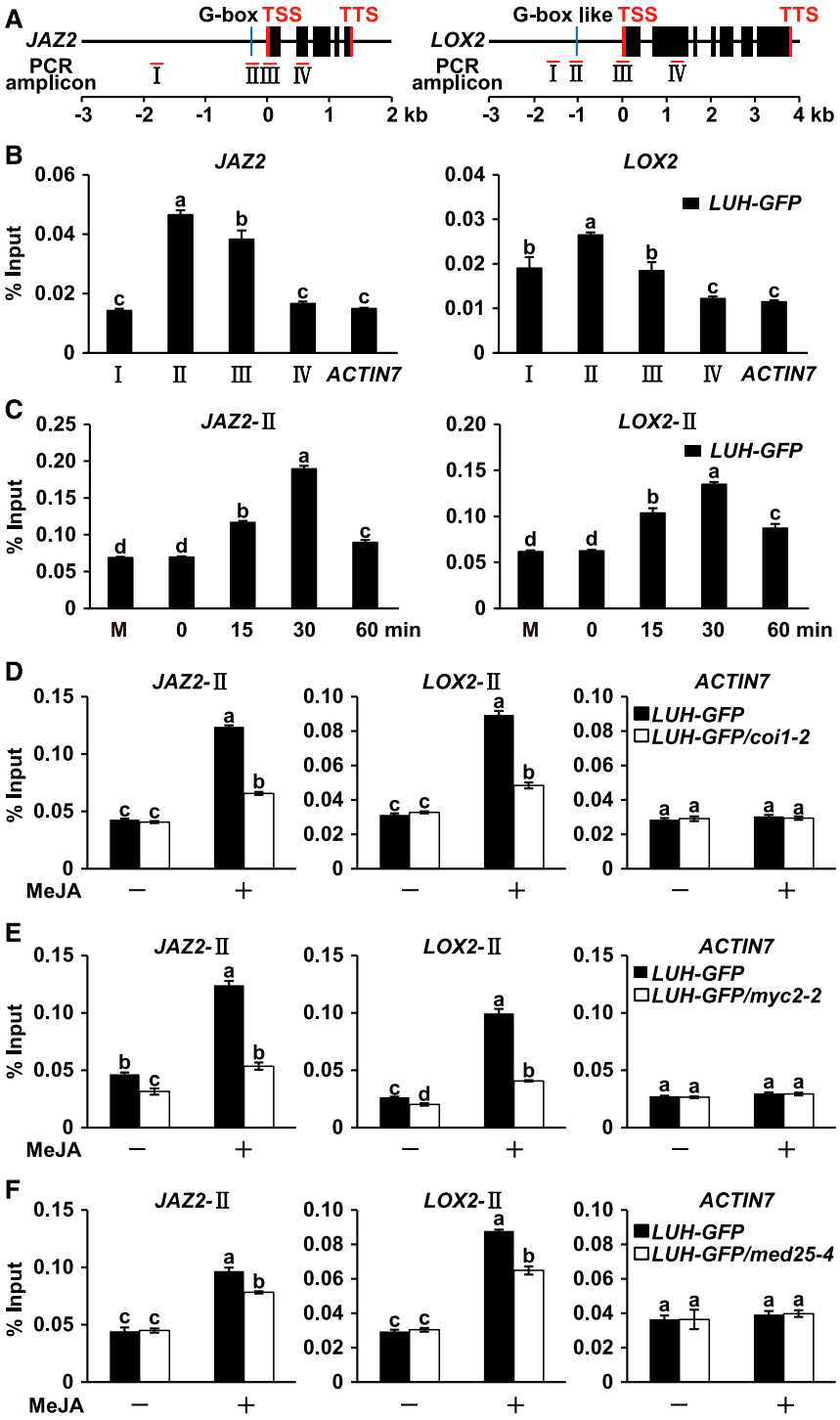

Figure 4. LUH Is Recruited to MYC2 Target Promoters in a MED25-Dependent Manner.

(A) Schematic diagrams of *JAZ2*, *LOX2*, and PCR amplicons (I, II, III, and IV) used for ChIP-qPCR. Positions of the TSS (0 kb) and transcription termination site (TTS) are indicated. Black boxes, exons; lines, noncoding regions.

(B) ChIP-qPCR analysis showing the enrichment of LUH at the promoter regions of *JAZ2* and *LOX2* in 10-d-old *LUH-GFP* seedlings without MeJA treatment.

(C) ChIP-qPCR analysis showing the enrichment of LUH at the G-boxes of *JAZ2* and *LOX2* promoters in 10-d-old *LUH-GFP* seedlings treated with either 0.1% (v/v) ethanol for 30 min (mock, M) or 100 μM MeJA for the indicated times before crosslinking.

(D) to **(F)** ChIP-qPCR analysis showing the enrichment of LUH at the G-boxes of *JAZ2* and *LOX2* promoters in the indicated plants treated with or without 100 μM MeJA for 30 min before crosslinking. For **(B)** to **(F)**, chromatin of each sample was immunoprecipitated using an anti-GFP antibody. Precipitated DNA was quantified by qPCR, and DNA enrichment is displayed as a percentage of input DNA. *ACTIN7* was used as a nonspecific target gene. Data are presented as mean ± SD. Different letters indicate significant difference at $P < 0.05$ ($n = 3$, one-way ANOVA, Tukey post test, three independent experiments; Supplemental File).

promoters of *JAZ2* and *LOX2*. ChIP-qPCR assays showed that MeJA-induced enrichment of LUH at the G-boxes of *JAZ2* and *LOX2* in *myc2-2* mutants was significantly lower than in the wild-type plants (Figures 4A and 4E). These results, together with the finding that the *myc2-2* mutation had a negligible effect on LUH protein levels before and after MeJA treatment (Supplemental Figure 5E), indicate that MYC2 regulates the enrichment of LUH at its target gene promoters. Additionally, ChIP-qPCR assays using *med25-4* transgenics revealed that MeJA-induced enrichment of LUH at the G-boxes of *JAZ2* and *LOX2* was significantly reduced in *med25-4* compared with the wild type (Figures 4A and 4F). These results, together with the finding that the *med25-4* mutation had a negligible effect on LUH protein levels (Supplemental Figure 5F), indicate that the enrichment of LUH at MYC2 target promoters is also regulated by MED25.

Collectively, these results reveal that JA signaling regulates the recruitment of LUH to MYC2 target promoters in a MYC2- and MED25-dependent manner.

LUH–HAC1 Interaction Is Required for MeJA-Induced Recruitment of HAC1 to the MYC2 Target Promoter

The role of LUH in promoting JA-induced activation of MYC2 prompted us to test the possibility that this function may be achieved by recruiting histone-modifying enzymes that activate gene transcription. To test this possibility, we performed Y2H assays to screen potential interactions between LUH and proteins involved in the JA signaling pathway, including HAC1, GENERAL CONTROL NONDEREPRESSIBLE5 (GCN5), and SET DOMAIN GROUP 8 (SDG8; Berr et al., 2010; Gimenez-Ibanez et al., 2015; An et al., 2017). The LUH protein preferentially interacted with HAC1, but not with GCN5 or SDG8 (Figure 5A). Additionally, no interaction was detected between LUG and HAC1 or other epigenetic regulators (Figure 5A), implying that the mechanism of action of LUG in activating MYC2 is distinct from that of LUH.

The Y2H-based domain mapping assays indicated that the LUH fragment spanning amino acids 373 to 499 ($LUH^{373-499}$), hereafter referred as the MD, but not the Q-rich domain, was involved in the LUH–HAC1 interaction (Supplemental Figure 7A). Additionally, Y2H assays showed that the N-terminal region of HAC1, containing the kinase-inducible domain-interacting (KIX) domain, TAZ-type zinc-finger (Znf-TAZ) domain, and plant homeodomain (PHD), is involved in LUH–HAC1 interaction (Supplemental Figure 7B).

To determine whether LUH interacts with HAC1 in planta, we generated *Pro35S*:*LUH-myc* (*LUH-myc*) plants expressing the coding sequence of *LUH* fused with *myc* under the control of the *Cauliflower mosaic virus* 35S promoter. Co-IP assays using *LUH-myc* plants and an anti-HAC1 antibody (An et al., 2017) showed that endogenous HAC1 was pulled down by LUH-myc (Figure 5B), indicating that HAC1 associates with LUH in vivo. Parallel experiments revealed that MeJA had a negligible effect on LUH–HAC1 interaction in the 1-h time frame tested (Figure 5B).

Our recent work showed that HAC1 is recruited to MYC2 target promoters during JA signaling (An et al., 2017). To test whether LUH is required for the JA-induced recruitment of HAC1 to MYC2 target promoters, we performed ChIP-qPCR assays using *HAC1-GFP* plants (An et al., 2017) and an anti-GFP antibody. Results showed that MeJA-induced enrichment of HAC1-GFP to the G-boxes of *JAZ2* and *LOX2* was substantially reduced in *luh-4* mutants in which the protein level of HAC1-GFP was not affected (Figures 5C and 5D; Supplemental Figure 8A). This indicated that the recruitment of HAC1 to MYC2 target promoters strictly depends on functional LUH.

Because HAC1 selectively regulates H3K9ac, an epigenetic mark for active gene transcription (Earley et al., 2007; An et al., 2017), we further investigated the impact of LUH on the level of H3K9ac epigenetic mark in MYC2 target promoters. ChIP-qPCR assays showed that the level of H3K9ac modification in the G-boxes of *JAZ2* and *LOX2* was significantly reduced in *luh-4* mutants compared with the wild type (Figures 5C and 5E). These results, together with the finding that the *luh-4* mutation had a negligible effect on HAC1 protein levels before and after MeJA treatment (Supplemental Figure 8B), suggest that the *luh-4* mutation affects HAC1-dependent H3K9ac modification of MYC2 target promoters. Taken together, these results demonstrate that LUH functions with HAC1 to act as a transcriptional coactivator of MYC2 during JA signaling.

LUH Enhances MED25–HAC1 Interaction during JA Signaling

Our finding that LUH determines the function of HAC1 and its enrichment at MYC2 target promoters raised the possibility that LUH may also affect the recruitment of MED25 to the same gene promoters, as MED25 physically and functionally interacts with HAC1 when bound to MYC2 target promoters (An et al., 2017). ChIP-qPCR assays revealed that, compared with the wild type, the MeJA-induced recruitment of MED25-myc to the G-boxes of *JAZ2* and *LOX2* was significantly reduced in *luh-4* mutants in which the protein level of MED25-myc is unchanged (Figures 6A and 6B; Supplemental Figure 8C). This indicated that LUH facilitates JA-induced recruitment of MED25 to MYC2 target promoters. These results, together with those showing JA-induced recruitment of LUH in a MED25-dependent manner (Figure 4F), suggest a positive feedback loop between LUH and MED25 for their recruitment to MYC2 target promoters.

Considering that LUH uses different domains, including the Q-rich and MD domains, to interact with MED25 and HAC1, respectively, we investigated whether LUH promotes the interaction between these MYC2 coactivators using Co-IP experiments with *MED25-myc* and *MED25-myc*/*luh-4* transgenic plants. In the wild-type background, the ability of MED25-myc to pull down endogenous HAC1 increased following MeJA treatment, suggesting that hormone elicitation enhances MED25–HAC1 interaction (Figure 6C). In the *luh-4* background, however, the effect of MeJA on MED25–HAC1 interaction was negligible (Figure 6C), suggesting that LUH plays an important role in the MeJA-induced enhancement of the MED25–HAC1 interaction. Taken together, these results suggest that LUH functions with both HAC1 and MED25 to act as a transcriptional coactivator of MYC2.

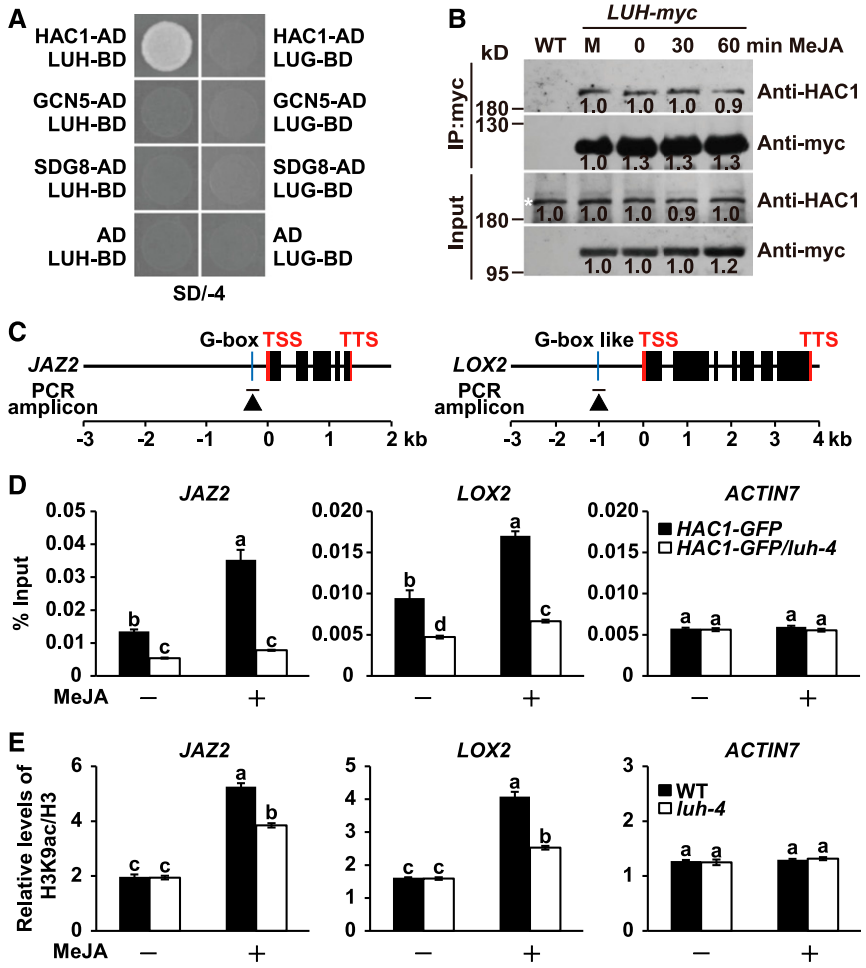

Figure 5. LUH Interacts with HAC1 and Determines the Enrichment of HAC1 at MYC2 Target Promoters.

(A) Y2H assays examining interactions between GAL4 BD fusions of LUH and LUG and GAL4 AD fusions of HAC1, GCN5, and SDG8. The transformed yeast cells were plated on SD/-4 medium. The empty AD vector was used as a negative control.

(B) Co-IP assays to verify the in vivo interaction between LUH and HAC1. Ten-day-old *LUH-myc* seedlings were treated with 0.1% (v/v) ethanol for 60 min (mock, M) or 100 μM MeJA for the indicated times. The wild-type (WT) seedlings were used as negative controls. Protein from each sample was immunoprecipitated using an anti-myc antibody and immunoblotted using an anti-HAC1 antibody. The asterisk indicates the position of HAC1. Bands were quantified using ImageJ, and relative levels are shown under each band. For **(A)** and **(B)**, experiments were repeated at least three times with similar results.

(C) Schematic diagram of *JAZ2*, *LOX2*, and PCR amplicons (black triangles) used for ChIP-qPCR. Positions of the TSS (0 kb) and transcription termination site (TTS) are indicated. Black boxes, exons; lines, noncoding sequences.

(D) ChIP-qPCR analysis showing the enrichment of HAC1 at the G-boxes of *JAZ2* and *LOX2* promoters in 10-d-old *HAC1-GFP* and *HAC1-GFP/luh-4* seedlings treated with or without 100 μM MeJA for 30 min before crosslinking. Chromatin of each sample was immunoprecipitated using an anti-GFP antibody. Precipitated DNA was quantified by qPCR and DNA enrichment is displayed as a percentage of input DNA.

(E) ChIP-qPCR analysis showing the enrichment of H3K9ac at the G-boxes of *JAZ2* and *LOX2* promoters in the 10-d-old wild-type (WT) and *luh-4* seedlings treated with or without 100 μM MeJA for 30 min before crosslinking. Chromatin of each sample was immunoprecipitated using anti-H3 and anti-H3K9ac antibodies. Precipitated DNA was quantified by qPCR, and H3K9ac levels are normalized to H3. For **(D)** and **(E)**, *ACTIN7* was used as a nonspecific target gene. Data are presented as mean ± SD. Different letters indicate significant difference at $P < 0.05$ ($n = 3$, one-way ANOVA, Tukey post test, three independent experiments; Supplemental File).

LUH Enhances MED25–MYC2 Interaction during JA Signaling

We recently showed that hormone elicitation enhances the MED25–MYC2 interaction (An et al., 2017). In this study, we showed that LUH interacts with MED25 and HAC1 via distinct domains. Together, these data suggest the possibility that LUH is involved in hormone-induced enhancement of MED25–MYC2 interaction. To test this possibility, we introduced the *MYC2-GFP* fusion construct (Zhai et al., 2013) into the *luh-4* mutant background and performed Co-IP experiments to evaluate the ability of MYC2-GFP to pull down native MED25 in *luh-4* mutants compared with the wild type. Our results showed that MeJA treatment increased the ability of MYC2-GFP to pull down MED25 after 1 h

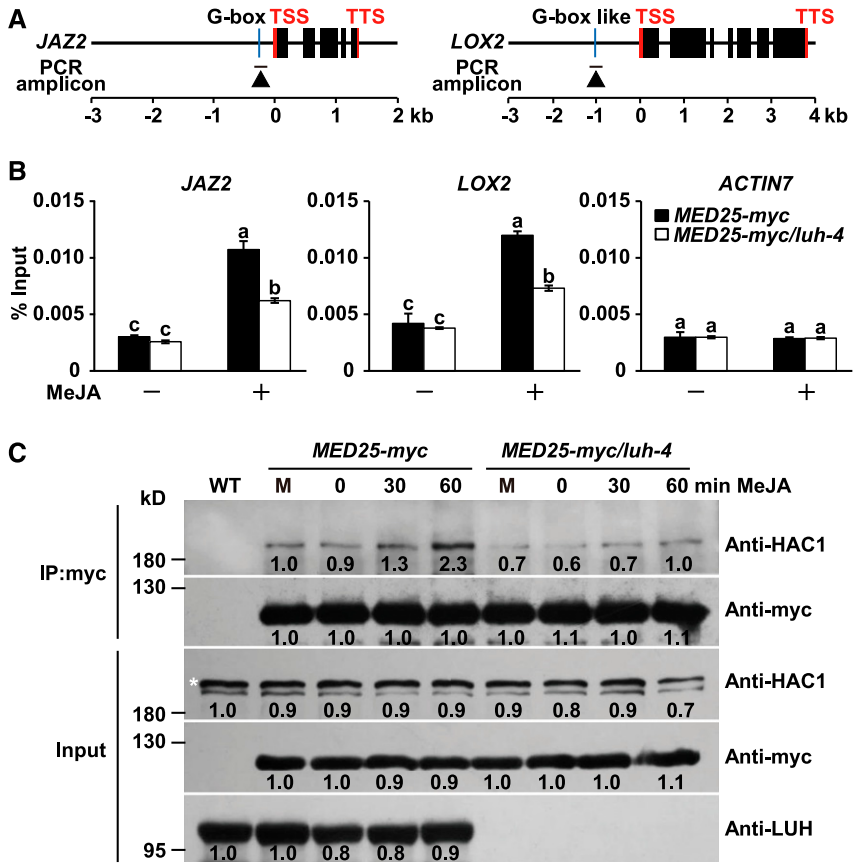

Figure 6. Depletion of LUH Reduces MeJA-Induced Recruitment of MED25 to MYC2 Target Promoters and Impairs MED25–HAC1 Interaction.

(A) Schematic diagram of *JAZ2*, *LOX2*, and PCR amplicons indicated as black triangles used for ChIP-qPCR. Positions of the TSS (0 kb) and transcription termination site (TTS) are indicated.

(B) ChIP-qPCR analysis showing the enrichment of MED25 at the G-boxes of *JAZ2* and *LOX2* promoters in 10-d-old *MED25-myc* and *MED25-myc/luh-4* seedlings treated with or without 100 μM MeJA for 30 min before crosslinking. Chromatin of each sample was immunoprecipitated using an anti-myc antibody. Precipitated DNA was quantified by qPCR and DNA enrichment is displayed as a percentage of input DNA. *ACTIN7* was used as a nonspecific target gene. Data are presented as mean ± SD. Different letters indicate significant difference at $P < 0.05$ ($n = 3$, one-way ANOVA, Tukey post test, three independent experiments; Supplemental File).

(C) Co-IP assays showing the effect of LUH depletion on the interaction between MED25 and HAC1 in response to MeJA treatment. Ten-day-old *MED25-myc* and *MED25-myc/luh-4* seedlings were treated with 0.1% (v/v) ethanol for 60 min (mock, M) or 100 μM MeJA for the indicated times. The wild-type (WT) seedlings were used as negative controls. Protein from each sample was immunoprecipitated using anti-myc antibody and immunoblotted using anti-HAC1 antibody. The asterisk indicates the position of HAC1. Bands were quantified using ImageJ, and relative levels are shown under each band. These experiments were repeated for at least three times with similar results. IP, immunoprecipitation.

markedly in the wild-type plants but only mildly in *luh-4* mutants (Figure 7A), suggesting that LUH plays a critical role in promoting MED25–MYC2 interaction during JA signaling.

DISCUSSION

In summary, we propose a working model to explain the function of LUH in promoting MYC2-dependent activation of JA-responsive genes, for example, *JAZ2* and *LOX2* (Figure 7B). In the resting stage, JAZ proteins recruit the corepressor TPL to inhibit MYC2-dependent activation of *JAZ2* and *LOX2* (Figure 7B). Following hormone-dependent degradation of JAZ repressors, MED25 interacts with LUH, thereby recruiting LUH (this study) and HAC1 (An et al., 2017) to *JAZ2* and *LOX2* promoters. Subsequently, LUH facilitates the recruitment of co-activators MED25 and HAC1 to *JAZ2* and *LOX2* promoters. Moreover, LUH plays a positive role in regulating hormone-mediated enhancement of the MED25–MYC2 and MED25–HAC1 interactions (Figure 7B), which promote *JAZ2* and *LOX2* activation. Our model highlights a mechanistic function of LUH in coordinating the actions of the master transcription factor MYC2 and its coactivators MED25 and HAC1 and can explain the activation of other JA-responsive genes by LUH. Considering that MED25, LUH, and HAC1 interact with each other, it is also possible that these coactivators form a complex before being recruited to MYC2 target promoters.

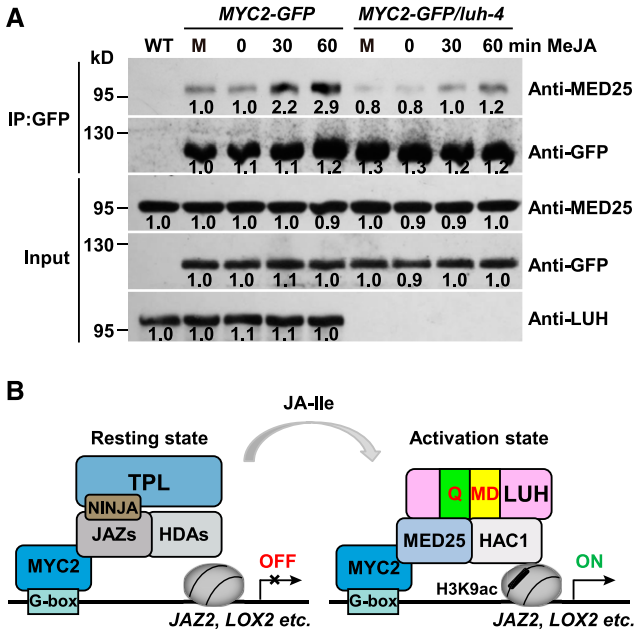

Figure 7. LUH Cooperates with MED25 and HAC1 During JA-Triggered Activation of MYC2.

(A) Co-IP assays showing the effect of LUH depletion on the interaction between MYC2 and MED25 in response to MeJA. Ten-day-old *MYC2-GFP* and *MYC2-GFP/luh-4* seedlings were treated with 0.1% (v/v) ethanol for 60 min (mock, M) or 100 μM MeJA for the indicated times. The wild-type (WT) seedlings were used as negative controls. Protein from each sample was immunoprecipitated using anti-GFP antibody and immunoblotted using anti-MED25 antibody. Bands were quantified using ImageJ, and relative levels are shown under each band. Experiments were repeated at least three times with similar results. IP, immunoprecipitation.

(B) Schematic of the proposed model explaining the role of LUH in the interaction between MED25 and HAC1 during JA-triggered activation of MYC2. In this model, MED25 physically interacts with LUH and recruits it to the promoters of *JAZ2* and *LOX2*. LUH then recruits HAC1 through direct interaction and promotes MeJA-induced interaction of MED25 with HAC1 and MYC2. Thus, LUH acts as a scaffold to bind the coactivators MED25 and HAC1 during JA-triggered activation of MYC2. HDA, histone deacetylase.

Gro proteins in *Drosophila* and their homologs in mammals and yeast are highly conserved transcriptional corepressors containing Trp and Asp (WD) repeats and Gln (Q)-rich domains (Chen and Courey, 2000; Jennings and Ish-Horowicz, 2008). It is generally believed that the Gro/Tup1 transcriptional corepressors function by generating a repressed chromatin state of genetic loci that control major developmental or signaling decisions. In Arabidopsis, Gro/Tup1-like proteins constitute a small family of 13 members, which are grouped into two distinct subclasses represented by TPL/TPR and LUG/LUH (Liu and Karmarkar, 2008; Lee and Golz, 2012). A growing body of evidence suggests that plant TPL/TPR proteins act as transcriptional corepressors and regulate a wide range of developmental processes and hormone signaling pathways through a conserved mechanism (Long et al., 2006; Szemenyei et al., 2008; Pauwels et al., 2010; Causier et al., 2012; Krogan et al., 2012; Jiang et al., 2013; Tao et al., 2013; Wang et al., 2013; Oh et al., 2014; Pi et al., 2015). In the case of JA signaling, TPL is recruited to MYC2 target promoters either by ethylene-responsive element binding factor–associated amphiphilic repression (EAR) motif-containing JAZ proteins or by the adaptor protein NINJA. Both interactions depend on the presence of a TPL binding EAR repression motif (Pauwels et al., 2010). In turn, TPL is predicted to recruit chromatin modification factors to repress target gene expression (Liu and Karmarkar, 2008; Krogan et al., 2012; Lee and Golz, 2012). Similarly, LUG/LUH subclass proteins act as transcriptional corepressors to regulate diverse physiological processes, including floral development, pectin structure, and seed germination (Liu and Meyerowitz, 1995; Conner and Liu, 2000; Sridhar et al., 2004; Sitaraman et al., 2008; Stahle et al., 2009; Grigorova et al., 2011; Huang et al., 2011; Walker et al., 2011; Lee et al., 2015).

In contrast to previous reports, this study provides compelling evidence supporting the role of Arabidopsis LUH as an important component of the MMC, which plays a critical role in activating MYC2-mediated transcription of JA-responsive genes. The deletion of *LUH* impaired the MYC2-mediated transcription of JA-responsive genes. Additionally, LUH physically interacted with and coordinated the MYC2 coactivators MED25 and HAC1. Moreover, LUH played a critical role in JA-induced enhancement of MED25–HAC1 and MED25–MYC2 interactions. Together, these results suggest that LUH acts as a transcriptional coactivator of JA signaling, unlike other Gro/Tup1 proteins that act as transcriptional corepressors, showing that different members of the Gro/Tup1 family play distinct roles in the same signaling pathway.

The antagonistic roles of LUH and TPL in the JA signaling pathway might be attributed to their distinct protein domains, which are required to bind to or recruit different partners. For example, the Q-rich domain of LUH, which is required for binding to the coactivator MED25, is absent in TPL (Supplemental Figure 1). Similarly, the C-terminal to LisH domain within the N terminus of TPL, which is required for binding to JAZ repressors and the adaptor protein NINJA, is loosely conserved in LUH (Supplemental Figure 1; Pauwels et al., 2010; Ke et al., 2015). In addition, the MD of LUH, which is required for interaction with the coactivator HAC1, is poorly conserved in TPL (Supplemental Figure 1).

Our data provide insight into the mechanism underlying the function of LUH as a coactivator. Analysis of the repressive mechanisms used by TPL proteins and LUG indicated that one such mechanism used by these corepressors is the recruitment of histone deacetylases to reversibly modify histone acetylation (Gonzalez et al., 2007; Krogan et al., 2012; Wang et al., 2013; Pi et al., 2015). Our biochemical analyses established a direct interaction between LUH and HAC1 (Figure 5), a histone acetyltransferase that facilitates the transcriptional regulation of MYC2 by altering the level of H3K9ac epigenetic mark in MYC2 target promoters (An et al., 2017). The significance of this interaction is evident from the results of ChIP analysis of HAC1 in the *luh-4* mutant, demonstrating that LUH recruits HAC1 to MYC2 target promoters. The level of H3K9ac modification in these MYC2 target promoters was consistently and significantly reduced in the *luh-4* mutant compared with the wild type (Figure 5). Overall, these results suggest that the LUH–HAC1 complex promotes H3K9ac in the promoter region of MYC2

target genes as part of a gene-activation mechanism, supporting H3 acetylation as a conserved marker of active gene transcription (Earley et al., 2007).

While hormone-mediated protein–protein interactions are frequently involved in JA-Ile perception (Sheard et al., 2010) and JAZ-mediated repression of MYC transcription factors (Zhang et al., 2015), we report here that LUH is involved in protein–protein interactions that play a pivotal role in regulating the epigenetic activation of MYC2-dependent transcription of JA-responsive genes. Specifically, LUH acts as a scaffold for binding MED25 and HAC1, both of which are MYC2 coactivators, and it plays a critical role in hormone-induced enhancement of MED25–HAC1 and MED25–MYC2 interactions. Future structural studies are expected to provide further insight into the role of LUH in hormone-mediated enhancement of protein–protein interactions between MYC2 and its multiple coactivators.

Several lines of evidence support the redundant functions of LUG and LUH in activating MYC2-mediated transcription of JA-responsive genes. First, LUH and LUG have high sequence similarity, and both proteins physically interacted with the MYC2 coactivator MED25. Second, *luh* or *lug* single mutants showed a relatively weak JA signaling deficiency, and *lug/+* heterozygous mutants enhanced the JA signaling deficiency of *luh*. Finally, unlike LUH, LUG did not physically interact with the epigenetic coactivator HAC1, implying that LUG might interact with epigenetic co-activator(s) other than HAC1. Together, these observations support a scenario in which LUG and LUH perform overlapping functions in activating MYC2-mediated transcription of JA-responsive genes, although via distinct mechanisms of action. Consistent with this hypothesis, it has been shown that LUH and LUG perform partially redundant functions in regulating embryo and floral development (Sitaraman et al., 2008). In future studies, it will be of significance both to identify the epigenetic partners of LUG that activate MYC2-mediated expression of JA-responsive genes and to elucidate their underlying mechanisms of action.

Notably, we found that the effects of LUH and LUG on JA-responsive gene expression are relatively weak compared with those of MYC2 (Lorenzo et al., 2004; Dombrecht et al., 2007) and MED25 (Kidd et al., 2009; Chen et al., 2012). A plausible explanation for this interesting observation is that these MMC components play different roles in the activation of JA-responsive gene transcription: whereas MYC2 is responsible for turning on the transcription and MED25 is responsible for recruiting the Pol II transcriptional machinery, LUH and LUG fine tune transcription by regulating the recruitment of HAC1 and other possible epigenetic factors.

METHODS

Plant Materials and Growth Conditions

Arabidopsis (*Arabidopsis thaliana*) ecotype Columbia was used as the wild type. The following transgenic plant materials were used in this study and have been described previously: *MED25-myc* (Chen et al., 2012), *MYC2-myc* (Chen et al., 2011), *luh-3* (Sitaraman et al., 2008), *luh-4* (Stahle et al., 2009), *lug-444* (Stahle et al., 2009), *coi1-2* (Xu et al., 2002), *myc2-2* (Boter et al., 2004), *med25-4* (Chen et al., 2012), *MYC2-GFP* (Zhai et al., 2013), and *HAC1-GFP* (An et al., 2017). The *HAC1-GFP*, *MED25-myc*, and *MYC2-GFP* transgenes were introduced into the *luh-4* background via crossing. Homozygous plants were selected by genotyping. Homozygous *lug-444* mutants were identified from an F2 population segregating for the *lug-444* mutation either by genotyping of 10-d-old seedlings or by scoring the reported incised rosette leaves of 21-d-old plants (Stahle et al., 2009). The *luh-4 lug-444/+* (homozygous for *luh-4* and heterozygous for *lug-444*) mutants were identified from populations segregating for both *luh-4* and *lug-444* mutations by scoring the characteristic polarity defects of cotyledons of 10-d-old seedlings and leaves of 21-d-old plants (Sitaraman et al., 2008; Stahle et al., 2009). Arabidopsis plants used for protoplast preparation, insect feeding, and the pathogen infection assays were grown in soil (vermiculite:nutrition soil ratio of 1:1) at 22°C with a short-day (10-h light/14-h dark) photoperiod for 4 weeks. Other Arabidopsis plants were grown at 22°C under a long-day (16 h light/8 h dark) photoperiod (light intensity of 120 μmol photons m^{-2} s^{-1}).

Plasmid Construction and Plant Transformation

To construct *ProLUH:LUH-GFP* (*LUH-GFP*) and *ProLUG:LUG-GFP* (*LUG-GFP*) plasmids, the promoter and coding sequences of *LUH* and *LUG* were amplified by PCR and cloned into *pCAMBIA1300-GFP* (An et al., 2017). To construct the *Pro35S:LUH-myc* (*LUH-myc*) plasmid, the coding sequence of *LUH* was PCR amplified, cloned into *pENTR* using a pENTR Directional TOPO Cloning Kit (Invitrogen), and recombined with the binary vector *PGWB17* (Nakagawa et al., 2007). Primers used for plasmid construction are listed in Supplemental Table 2. These constructs were transformed into *Agrobacterium tumefaciens* strain GV3101 and then the transformed GV3101 cells were used to generate transgenic Arabidopsis plants using the floral dip method (Clough and Bent, 1998). Transformants were selected based on their resistance to hygromycin. Homozygous T3 or T4 lines were used in various experiments. *LUH-GFP* was introduced into the *coi1-2*, *myc2-2*, or *med25-4* mutant background by crossing, and homozygous plants were selected by genotyping.

Purification of MED25-Containing Protein Complexes and Tandem Mass Spectrometric Analysis

Samples (5 g) of 10-d-old *MED25-myc* seedlings were harvested, ground in liquid nitrogen, and lysed with 10 mL of ice-cold extraction buffer (50 mM Tris-HCl, pH 7.5, 150 mM NaCl, 5 mM EDTA, 0.1% [v/v] Triton X-100, 0.2% [v/v] Nonidet P-40, 0.6 mM phenylmethylsulfonyl fluoride [PMSF], and 20 μM MG132 with Roche protease inhibitor cocktail). After vortexing vigorously for 30 s, the samples were centrifuged at 13,000*g* for 10 min at 4°C. For each sample, 30 μL of the supernatant was subjected to immunoblot analysis, and the remainder was incubated with 50 μL of myc antibody–bound agarose beads (MBL, MEDICAL & BIOLOGICAL LABORATORIES CO., LTD.) for 4 h at 4°C with gentle shaking. Beads were collected and washed four times with extraction buffer and once with 50 mM Tris-HCl, pH 7.5. The precipitate was eluted using 1× SDS protein loading buffer and separated using 10% SDS-PAGE. The gel was stained with Thermo GelCode Blue Safe Protein Stain and washed with double distilled water.

The gel (containing the samples) was cut into small pieces and destained in buffer containing 25 mM ammonium bicarbonate and 50% (v/v) acetonitrile, pH 8.0. Proteins were reduced with 10 mM DTT at 37°C for 1 h and alkylated with 25 mM iodoacetamide at room temperature for 1 h in darkness. In-solution trypsin digestion was performed at 37°C overnight using a trypsin:substrate ratio of 1:50. Peptides were extracted from the gel with buffers containing 5% (v/v) trifluoroacetic acid and 50% (v/v) acetonitrile, pH 0.5, after two rounds of ultrasonication. Liquids were freeze dried in a SpeedVac, and peptides were resolubilized in 0.1% (v/v) formic acid and filtered through a 0.45-μm centrifugal filter.

Peptides were analyzed using a TripleTOF 5600 mass spectrometer (AB SCIEX) coupled to an online Eksigent nanoLC Ultra HPLC system in information-dependent mode. The LC gradient (solvent A = 0.1% formic acid in water; solvent B = 0.1% formic acid in acetonitrile) used for sample elution was 5 to 90% solvent B for 90 min at a flow rate of 300 nL min^{-1}.

Peptides were identified from the tandem mass spectrometric spectra using ProteinPilot v4.2 by searching against the Arabidopsis International Protein Index database. Carbamidomethylation of Cys residues was used as the fixed modification. Trypsin was specified as the proteolytic enzyme allowing two missed cleavage sites. Mass tolerance was set to 0.05 D, and the maximum FDR for proteins and peptides was set to 1%.

Y2H Assays

To verify the interactions of MED25 with LUH, LUG, and TPL, the coding sequences of *LUH* and its derivatives, *LUG*, and *TPL* were fused with the GAL4 AD in *pGADT7*, and those of *MED25* and its derivatives were fused with the GAL4 BD in *pGBKT7*. To investigate the interactions of LUH and LUG with MYC2, HAC1, GCN5, and SDG8, the coding sequences of *MYC2*, *HAC1* and its derivatives, *GCN5*, and *SDG8* were fused with the GAL4 AD in *pGADT7*, and the coding sequences of *LUH*, *LUG*, and *LUH* derivatives were fused with the GAL4 BD in *pGBKT7*. Primers used for generating these constructs are listed in Supplemental Table 2. Constructs used for the expression of MED25 derivatives and HAC1 derivatives have been described previously (Chen et al., 2012; An et al., 2017). Constructs used to test protein–protein interactions were cotransformed into yeast (*Saccharomyces cerevisiae*) strain AH109. Cotransformation of the empty *pGADT7* vector was used as a negative control. The presence of transgenes in yeast cells was confirmed by growth on plates containing solid synthetic defined (SD) media lacking Leu and Trp (SD/-2). To assess protein–protein interactions, the transformed yeast cells were suspended in liquid SD/-2 to an OD_{600} of 1.0. Samples (5 μL) of suspended yeast cells were spread on plates containing SD media lacking Ade, His, Leu, and Trp (SD/-4). Interactions were observed after 3 d of incubation at 30°C.

Antibody Generation

The coding sequences of *LUH* and *LUG* were PCR amplified from the wild-type cDNA using gene-specific primers (Supplemental Table 2). The resultant PCR products were cloned into vector *pGEX-4T-3* (Sigma-Aldrich) to express GST-LUH and GST-LUG protein fusion in *Escherichia coli* BL21 (DE3). The recombinant fusion proteins were purified with GST Bind Resin (Millipore) and used to raise polyclonal antibodies in mice. Anti-LUH and anti-LUG antibodies made in our institute were used in protein gel blotting at a final dilution of 1:2000.

In Vitro Pull-Down Assays

To produce the MBP-LUH fusion protein, the coding sequence of *LUH* was PCR amplified and cloned into *pMAL-c2X* (New England Biolabs). To produce GST-tagged $MED25^{MA}$ (GST-$MED25^{MA}$) protein, a *MED25* fragment spanning the MD and ACID domains (amino acids 227 to 680) was amplified and cloned into the *pGEX-4T-3* vector. Primers used for generating these constructs are listed in Supplemental Table 2. The recombinant vectors were transformed into *E. coli* BL21 (DE3) cells, and the fusion proteins were purified using amylose resin (New England Biolabs) or GST Bind Resin (Millipore). For each reaction, 15 μL of agarose beads (Millipore) bound with 1 μg of GST-$MED25^{MA}$ was incubated with 1 μg of MBP-LUH in 1 mL of reaction buffer (25 mM Tris-HCl, pH 7.5, 100 mM NaCl, 1 mM DTT, and Roche protease inhibitor cocktail) at 4°C for 1 h. Subsequently, the beads were collected and washed three times with washing buffer (25 mM Tris-HCl, pH 7.5, 150 mM NaCl, and 1 mM DTT). After washing, samples were denatured using SDS protein loading buffer and separated using SDS-PAGE. The MBP-LUH fusion protein was detected by immunoblotting with anti-MBP antibody (1:10,000; catalog no. E8032, New England Biolabs). Purified GST was used as a negative control. Five-microliter aliquots of GST and GST-$MED25^{MA}$ fusion proteins were separated by SDS-PAGE, and the staining of polyacrylamide gels with Coomassie Brilliant Blue R 250 was used as a loading control.

Immunoblot Analysis

Protein extraction and immunoblotting were performed according to standard protocols. Ten-day-old seedlings were ground into fine powders in liquid nitrogen and then transferred to extraction buffer (50 mM Tris-HCl, pH 7.5, 10 mM EDTA, pH 8.0, 150 mM NaCl, 50 mM DTT, 2% [v/v] Nonidet P-40, and Roche protease inhibitor cocktail). For immunoblot analysis, protein samples were boiled for 5 min after mixing with SDS protein loading buffer, separated by SDS-PAGE, and transferred to polyvinylidene fluoride membranes. Immunoblots were probed with anti-LUH antibody (1:2000; this study), or anti-GFP antibody (1:2000; catalog no. M20004, Abmart), or anti-HAC1 antibody (1:2,000; An et al., 2017), or anti-myc antibody (1:2000; catalog no. M20002, Abmart), and signals were quantified using ImageJ software (National Institutes of Health). Ponceau S–stained membranes were used as loading controls.

Co-IP Assays

Ten-day-old *MED25-myc* or *MYC2-myc* seedlings were treated with or without 100 μM MeJA for the indicated times. Each sample was collected, ground in liquid nitrogen, and used for protein extraction using extraction buffer (50 mM Tris-HCl, pH 7.5, 5 mM EDTA, pH 8.0, 150 mM NaCl, 0.1% [v/v] Triton X-100, 0.2% [v/v] Nonidet P-40, 0.6 mM PMSF, and 20 μM MG132 with Roche protease inhibitor cocktail). After protein extraction, 20 μL of protein G plus agarose beads (Santa Cruz Biotechnology) was added to the 2-mg extracts to reduce nonspecific immunoglobulin binding. After 1 h of incubation, the supernatant was transferred to a new tube. Myc antibody-bound agarose beads (MBL) were then added to each reaction for 4 h at 4°C. The wild-type seedlings were used as negative controls. The precipitated samples were washed at least four times with protein extraction buffer and then eluted by boiling the beads in SDS protein loading buffer for 5 min. Immunoblots were detected with an anti-LUH antibody (1:2000) and an anti-myc antibody (1:2000; catalog no. M20002, Abmart). To test the in vivo interaction of LUG and MED25, Co-IP assays were performed in a similar manner, using *MED25-myc* plants and anti-LUG antibody (1:2000). To test the in vivo interaction of HAC1 and LUH, Co-IP assays were performed, as described above, using *LUH-myc* plants and anti-HAC1 antibody (1:2000; An et al., 2017).

To test the effect of LUH on the interaction between MED25 and HAC1, Co-IP assays were performed using *MED25-myc* and *MED25-myc/luh-4* transgenic plants. Immunoblots were detected with an anti-HAC1 antibody (1:2000; An et al., 2017) and anti-myc antibody (1:2000; catalog no. M20002, Abmart).

To investigate the effect of LUH on the interaction between MYC2 and MED25, Co-IP assays were performed in a similar manner, using *MYC2-GFP*, *MYC2-GFP/luh-4* transgenic plants, except that the beads were protein A plus agarose beads (Santa Cruz Biotechnology) and GFP antibody-bound agarose beads (MBL). Immunoblots were detected with an anti-MED25 antibody (1:2000; Chen et al., 2012) and an anti-GFP antibody (1:2000; catalog no. M20004, Abmart). All the signals were quantified using ImageJ software.

RNA-Seq and Data Analysis

The 10-d-old wild-type and *luh-4* seedlings were treated with 100 μM MeJA for 1, 6, or 24 h. The untreated wild-type and *luh-4* seedlings were

used as controls. Seedlings from three biological replicates were collected for RNA extraction, and there were 24 independent samples in total. Total RNA of each sample was extracted using an RNeasy Plant Mini Kit (Qiagen) and treated with DNase I. The quality of the total RNA was assessed using a NanoDrop spectrophotometer and an Agilent 2100 Bioanalyzer. For each sample, 3 μg of total RNA was used to construct the Illumina sequencing libraries according to the manufacturer's instructions. The libraries were sequenced using the Illumina HiSeq 2500 platform (Berry Genomics) to generate high-quality paired-end reads of 150 nucleotides.

The Arabidopsis genome sequences and annotated gene models were downloaded from TAIR10 (The Arabidopsis Information Resource, version 10; www.arabidopsis.org/). Raw sequencing reads were first processed to remove adaptors and low-quality bases and then aligned to the genome sequences using STAR (2.5.2b), with the maximum allowed intron size set as 5000 nucleotides. The mapping quality and saturation analysis were performed using RSeQC (Wang et al., 2012). Differentially expressed genes were identified using DESeq2 (Love et al., 2014) as those with an absolute fold change > 1.5 and FDR-adjusted $P < 0.05$. Genes with more than a 1.5-fold change of expression (FDR-adjusted $P < 0.05$) between any time after MeJA treatment (1, 6, or 24 h) and untreated control were defined as MeJA-regulated genes in different genotypes. Genes with more than a 1.5-fold change of expression (FDR-adjusted $P < 0.05$) at any time after MeJA treatment (1, 6, or 24 h) between the wild-type and *luh-4* were defined as LUH-regulated genes. MeJA- and LUH-coregulated genes were selected for further investigation. GO enrichment analyses were performed using clusterProfiler (Yu et al., 2012). GO term enrichment is shown by the most specific subclass in the enrichment analysis. Comparison analysis and plots were performed using in-house transcripts based on the Python and R programming languages.

Transient Expression Assays in Arabidopsis Protoplasts

For the transient transcriptional activity assays, the 1745-bp promoter sequence of *LOX2* was amplified from genomic DNA and cloned into the *pGreenII 0800-LUC* (Hellens et al., 2005) vector to use as a reporter. The *Renilla luciferase* (*REN*) gene under the control of the cauliflower 35S promoter in the *pGreenII 0800-LUC* vector was used as the internal control. The coding sequences of *MYC2*, *LUH*, and *GFP* were cloned into the *pUC19-35S-HA-RBS* vector (Li et al., 2005) under the control of the 35S promoter and were used as effectors. Primers used for generating these constructs are listed in Supplemental Table 2. Arabidopsis mesophyll protoplasts were prepared and transfected as described previously by Yoo et al. (2007). Firefly LUC and REN activities were measured using the Dual-LUC Reporter Assay System (Promega) following the manufacturer's instructions, and LUC:REN ratios were calculated and presented. Data from three independent biological replicates were collected, and error bars represent the SD from three biological replicates.

Insect Feeding Assays with *Spodoptera exigua*

Insect feeding assays were performed as described previously (Hu et al., 2013; Song et al., 2013), with minor modifications. *S. exigua* eggs were hatched at 27°C. The third-instar *S. exigua* larvae were transferred to a Petri dish and starved for 12 h before participating in the feeding experiment. Forty-five mature rosette leaves of similar size from 4-week-old plants for each genotype were placed in plastic Petri dishes (150 mm) containing 1% (w/v) phytagel. Fifteen third-instar *S. exigua* larvae were weighed and reared on the leaves in one Petri dish for each genotype in three independent replicates. The *S. exigua* larvae were grown in the Petri dish for 4 d. The leaves in each Petri dish were replaced by 45 fresh leaves every 2 d. Four days after feeding, the weight of the 15 larvae was measured. Data from three independent biological replicates were collected, and error bars represent the SD from three biological replicates.

Botrytis cinerea Inoculation Assays

B. cinerea B05.10 was grown on 2 × V8 agar (36% [v/v] V8 juice, 0.2% [w/v] $CaCO_3$, and 2% [w/v] Bacto-agar) for 14 d at 20°C under a 12-h photoperiod prior to spore collection. Spore suspensions were prepared by harvesting the spores in potato dextrose broth (catalog no. 254920, Becton, Dickinson and Company), filtering them through nylon mesh to remove hyphae, and adjusting the concentration to 5×10^5 spores/mL. *B. cinerea* inoculation of Arabidopsis plants was performed as described previously by Van Wees et al. (2013), with minor modifications. The central vein of leaves of 4-week-old Arabidopsis plants was inoculated with a single 5-μL droplet of a *B. cinerea* spore suspension at a concentration of 5×10^5 spores/mL. Next, the plants were incubated in a growth chamber with high humidity (90%). A similar experiment was performed using potato dextrose broth–spotted plants as a control. Photographs were taken at 3 d after inoculation, and the lesion sizes were recorded. Sixteen spotted leaves were harvested at 3 d after inoculation for spore counting as described previously by Van Wees et al. (2013), and the rest of the spotted leaves were harvested for RT-qPCR. Data from three independent biological replicates were collected, and error bars represent the SD from three biological replicates.

Anthocyanin Content Measurement

Anthocyanin content was measured as described previously (Deikman and Hammer, 1995). The preweighed 21-d-old Arabidopsis seedlings (50 mg) grown on half-strength Murashige and Skoog (MS) medium treated with or without 100 μM MeJA for 48 h were placed into 1 mL of extraction buffer (18% [v/v] 1-propanol, 1% [v/v] HCl, and 81% [v/v] water). The sample was then boiled for 3 min and incubated overnight at room temperature. Absorbance values (A_{535} and A_{650}) of the extraction solution were measured using a spectrophotometer. The anthocyanin content is presented as (A_{535} to A_{650}) g^{-1} fresh weight. Data from three independent biological replicates were collected, and error bars represent the SD from three biological replicates.

Root Growth Inhibition Assays

Seedlings were grown on half strength MS medium supplied with or without 20 μM JA (Sigma-Aldrich) for 10 d. The mean root length of 30 seedlings of each genotype was measured and presented. Data from three independent biological replicates were collected, and error bars represent the SD from three biological replicates.

ChIP-qPCR Assays

The 10-d-old wild-type, *luh-4*, *LUH-GFP*, *LUH-GFP/coi1-2*, *LUH-GFP/myc2-2*, *LUH-GFP/med25-4*, *HAC1-GFP*, *HAC1-GFP/luh-4*, *MED25-myc*, and *MED25-myc/luh-4* seedlings were treated with or without 100 μM MeJA for the indicated times, and 2 g of each sample was harvested and crosslinked in 1% (v/v) formaldehyde at room temperature for 10 min, followed by neutralization with 0.125 M Gly. The chromatin–protein complex was isolated, resuspended in lysis buffer (50 mM HEPES, pH 7.5, 150 mM NaCl, 1 mM EDTA, 1% [w/v] SDS, 1% [v/v] Triton X-100, 0.1% [w/v] sodium deoxycholate, and 1 mM PMSF, with 1× Roche protease inhibitor cocktail), and sheared by sonication to reduce the average DNA fragment size to ~500 bp. Next, 50 μL of the sheared chromatin was saved for use as the input control. Anti-GFP (ab290, Abcam), anti-myc (catalog no. 11667149001, Roche), anti-H3 (ab1791, Abcam), and anti-H3K9ac (ab10812, Abcam) antibodies were incubated with Dynabeads Protein G (Invitrogen) at 4°C for at least 6 h and added to the remaining chromatin for overnight incubation at 4°C. The immunoprecipitated chromatin–protein complex was sequentially washed with low-salt buffer (20 mM Tris-HCl, pH 8.0, 2 mM EDTA, 150 mM NaCl, 0.5% Triton X-100, and 0.2% SDS),

high-salt buffer (20 mM Tris-HCl, pH 8.0, 2 mM EDTA, 500 mM NaCl, 0.5% Triton X-100, and 0.2% SDS), LiCl buffer (10 mM Tris-HCl, pH 8.0, 1 mM EDTA, 0.25 M LiCl, 0.5% [v/v] Nonidet P-40, and 0.5% sodium deoxycholate), and TE buffer (10 mM Tris-HCl, pH 8.0, and 1 mM EDTA). After washing, the immunoprecipitated chromatin was eluted with elution buffer (1% SDS and 0.1 M $NaHCO_3$, pH 9.5). Protein–DNA crosslinks were reversed by incubating the immunoprecipitated complexes with 20 μL of 5 M NaCl overnight at 65°C. DNA was recovered using a QIAquick PCR Purification Kit (Qiagen) and analyzed by qPCR. The enrichment of DNA is shown as the percent of input, calculated by determining the immunoprecipitation efficiency at *JAZ2* and *LOX2* loci as the ratio of the amount of immunoprecipitated DNA to the normalized amount of starting material (percent of input DNA). H3K9ac levels are shown as the ratio of the amount of immunoprecipitated DNA assembled with H3K9ac to the amount of immunoprecipitated DNA assembled with H3. *ACTIN7* was used as a nonspecific target gene. Each PCR was repeated three times for technical replicates, and the mean value was recorded for each biological replicate. Data from three independent biological replicates were collected, and error bars represent the SD from three biological replicates. Primers for qPCR are listed in Supplemental Table 2.

RNA Extraction, RT, and RT-qPCR Assays

For RT-qPCR analyses of JA-responsive genes in the wild type, *luh-3*, and *luh-4*, total RNA was extracted from 10-d-old seedlings treated with or without 100 μM MeJA for the indicated times using TRIzol Reagent (Invitrogen). For RT-qPCR analysis of JA-responsive genes in the wild type, *luh-4*, *lug-444*, and *luh-4 lug-444*/+, total RNA was extracted from 21-d-old seedlings treated with or without 100 μM MeJA for the indicated times. cDNA was prepared from 2 μg of total RNA with SuperScript III reverse transcriptase (Invitrogen) and quantified on a Roche 480 cycler with the SYBR Green kit (Takara). The expression levels of target genes were normalized against *ACTIN7*. Each PCR analysis was repeated three times for technical replicates, and the mean value was recorded for each biological replicate. Data from three independent biological replicates were collected, and error bars represent the SD from three biological replicates. Primers are listed in Supplemental Table 2.

Accession Numbers

Sequence data from this article can be found in the Arabidopsis Genome Initiative under the following accession numbers: *LUH*, At2g32700; *LUG*, At4g32551; *TPL*, At1g15750; *MED25*, At1g25540; *MYC2*, At1g32640; *COI1*, At2g39940; *JAR1*, AT2g46370; *VSP2*, At5g24770; *PDF1.2*, At5g44420; *JAZ2*, At1g74950; *LOX2*, At3g45140; *HAC1*, At1979000; *SDG8*, At1g77300; *GCN5*, At3g54610; *ACTIN7*, At5g09810; *JAL23*, AT2g39330; *MBP1*, AT1g52040; *MBP2*, AT1g52030; *ORA59*, AT1g06160; *PDF1.2b*, AT2g26020; *PDF1.2c*, AT5g44430; *CYP71A12*, AT2g30750; *CYP71A13*, AT2g30770; *CYP71B15*, AT3g26830; *JMT*, AT1g19640; *MYB47*, AT1g18710; *PR1*, AT2g14610; *MYB95*, AT1g74430; *THI2.1*, AT1g72260; *WRKY38*, AT5g22570; *TSA1*, AT1g52410; *PDR12*, AT1g15520; *WAK1*, AT1g21250; *5PTASE11*, AT1g47510; *CRK36*, AT4g04490; *TPS03*, AT4g16740; *FAR5*, AT3g44550; *AOC1*, AT3g25760; *JAZ6*, AT1g72450; *LOX1*, AT1g55020; *VSP1*, AT5g24780. The raw sequence data reported in this article have been deposited in the Genome Sequence Archive (Wang et al., 2017) in Beijing Institute of Genomics (BIG) Data Center (BIG Data Center Members, 2019), BIG, Chinese Academy of Sciences, under accession number CRA001682 that is publicly accessible at http://bigd.big.ac.cn/gsa. Germplasm used included the T-DNA lines *luh-3* (SALK_107245) and *luh-4* (SALK_097509).

Supplemental Data

Supplemental Figure 1. Mapping of protein domains involved in LUH–MED25 interaction.

Supplemental Figure 2. Identification of *luh* mutants.

Supplemental Figure 3. Summary of the RNA-seq analysis.

Supplemental Figure 4. LUG interacts with MED25 in planta.

Supplemental Figure 5. Molecular characterization of *ProLUH:LUH-GFP* (*LUH-GFP*) transgenic plants.

Supplemental Figure 6. LUG is recruited to MYC2 target promoters.

Supplemental Figure 7. Mapping of protein domains involved in LUH–HAC1 interaction.

Supplemental Figure 8. Mutation of *LUH* has no effect on the levels of HAC1 and MED25.

Supplemental Table 1. *Arabidopsis thaliana* proteins identified as components of the MYC2–MED25 complex (MMC) using liquid chromatography-tandem mass spectrometry (LC-MS/MS).

Supplemental Table 2. Primers used in this study.

Supplemental Data Set 1. Genes upregulated in WT after MeJA treatment and genes whose expression is reduced in *luh-4* compared with WT treated with or without MeJA.

Supplemental Data Set 2. LUH- and MeJA-co-upregulated genes, GO analysis, and genes used in Figure 2B.

Supplemental Data Set 3. Genes downregulated in WT after MeJA treatment and genes whose expression is higher in *luh-4* compared with WT treated with or without MeJA.

Supplemental Data Set 4. LUH- and MeJA-co-downregulated genes and GO analysis.

Supplemental File. ANOVA analyses.

ACKNOWLEDGMENTS

This work was supported by the Strategic Priority Research Program of the Chinese Academy of Sciences (Grant XDB11030200), the Ministry of Science and Technology of China (Grant 2015CB942900), the National Natural Science Foundation of China (Grants 31730010 and 31770303), the Chinese Academy of Sciences Youth Innovation Promotion Association (Grant 2014082), and the Tai-Shan Scholar Program from the Shandong Provincial Government.

AUTHOR CONTRIBUTIONS

C.L. and Q.Z. designed the research. Y.Y., Q.Z., and C.A. performed the research. Y.Y., C.L., and Q.Z. analyzed data. Y.Y., Q.Z., and C.L. wrote the article.

Received February 20, 2019; revised May 24, 2019; accepted July 17, 2019; published July 18, 2019.

REFERENCES

Allen, B.L., and Taatjes, D.J. (2015). The Mediator complex: A central integrator of transcription. Nat. Rev. Mol. Cell Biol. **16:** 155–166.

An, C., Li, L., Zhai, Q., You, Y., Deng, L., Wu, F., Chen, R., Jiang, H., Wang, H., Chen, Q., and Li, C. (2017). Mediator subunit MED25 links the jasmonate receptor to transcriptionally active chromatin. Proc. Natl. Acad. Sci. USA **114:** E8930–E8939.

Bäckström, S., Elfving, N., Nilsson, R., Wingsle, G., and Björklund, S. (2007). Purification of a plant mediator from *Arabidopsis thaliana* identifies PFT1 as the Med25 subunit. Mol. Cell **26:** 717–729.

Bell, E., Creelman, R.A., and Mullet, J.E. (1995). A chloroplast lipoxygenase is required for wound-induced jasmonic acid accumulation in *Arabidopsis.* Proc. Natl. Acad. Sci. USA **92:** 8675–8679.

Berger, S., Bell, E., Sadka, A., and Mullet, J.E. (1995). *Arabidopsis thaliana Atvsp* is homologous to soybean *VspA* and *VspB*, genes encoding vegetative storage protein acid phosphatases, and is regulated similarly by methyl jasmonate, wounding, sugars, light and phosphate. Plant Mol. Biol. **27:** 933–942.

Berr, A., McCallum, E.J., Alioua, A., Heintz, D., Heitz, T., and Shen, W.H. (2010). Arabidopsis histone methyltransferase SET DOMAIN GROUP8 mediates induction of the jasmonate/ethylene pathway genes in plant defense response to necrotrophic fungi. Plant Physiol. **154:** 1403–1414.

BIG Data Center Members. (2019). Database resources of the BIG data center in 2019. Nucleic Acids Res. **47** (D1): D8–D14.

Boter, M., Ruíz-Rivero, O., Abdeen, A., and Prat, S. (2004). Conserved MYC transcription factors play a key role in jasmonate signaling both in tomato and *Arabidopsis.* Genes Dev. **18:** 1577–1591.

Browse, J. (2009). Jasmonate passes muster: A receptor and targets for the defense hormone. Annu. Rev. Plant Biol. **60:** 183–205.

Causier, B., Ashworth, M., Guo, W., and Davies, B. (2012). The TOPLESS interactome: A framework for gene repression in *Arabidopsis.* Plant Physiol. **158:** 423–438.

Çevik, V., Kidd, B.N., Zhang, P., Hill, C., Kiddle, S., Denby, K.J., Holub, E.B., Cahill, D.M., Manners, J.M., Schenk, P.M., Beynon, J., and Kazan, K. (2012). MEDIATOR25 acts as an integrative hub for the regulation of jasmonate-responsive gene expression in *Arabidopsis.* Plant Physiol. **160:** 541–555.

Chen, Q., et al. (2011). The basic helix-loop-helix transcription factor MYC2 directly represses *PLETHORA* expression during jasmonate-mediated modulation of the root stem cell niche in *Arabidopsis.* Plant Cell **23:** 3335–3352.

Chen, G., and Courey, A.J. (2000). Groucho/TLE family proteins and transcriptional repression. Gene **249:** 1–16.

Chen, R., Jiang, H., Li, L., Zhai, Q., Qi, L., Zhou, W., Liu, X., Li, H., Zheng, W., Sun, J., and Li, C. (2012). The Arabidopsis mediator subunit MED25 differentially regulates jasmonate and abscisic acid signaling through interacting with the MYC2 and ABI5 transcription factors. Plant Cell **24:** 2898–2916.

Chini, A., Fonseca, S., Fernández, G., Adie, B., Chico, J.M., Lorenzo, O., García-Casado, G., López-Vidriero, I., Lozano, F.M., Ponce, M.R., Micol, J.L., and Solano, R. (2007). The JAZ family of repressors is the missing link in jasmonate signalling. Nature **448:** 666–671.

Clough, S.J., and Bent, A.F. (1998). Floral dip: A simplified method for *Agrobacterium*-mediated transformation of *Arabidopsis thaliana.* Plant J. **16:** 735–743.

Conner, J., and Liu, Z. (2000). LEUNIG, a putative transcriptional corepressor that regulates *AGAMOUS* expression during flower development. Proc. Natl. Acad. Sci. USA **97:** 12902–12907.

Deikman, J., and Hammer, P.E. (1995). Induction of anthocyanin accumulation by cytokinins in *Arabidopsis thaliana.* Plant Physiol. **108:** 47–57.

Dombrecht, B., Xue, G.P., Sprague, S.J., Kirkegaard, J.A., Ross, J.J., Reid, J.B., Fitt, G.P., Sewelam, N., Schenk, P.M., Manners, J.M., and Kazan, K. (2007). MYC2 differentially modulates diverse jasmonate-dependent functions in *Arabidopsis.* Plant Cell **19:** 2225–2245.

Du, M., et al. (2017). MYC2 orchestrates a hierarchical transcriptional cascade that regulates jasmonate-mediated plant immunity in tomato. Plant Cell **29:** 1883–1906.

Earley, K.W., Shook, M.S., Brower-Toland, B., Hicks, L., and Pikaard, C.S. (2007). *In vitro* specificities of Arabidopsis co-activator histone acetyltransferases: Implications for histone hyperacetylation in gene activation. Plant J. **52:** 615–626.

Fernández-Calvo, P., et al. (2011). The Arabidopsis bHLH transcription factors MYC3 and MYC4 are targets of JAZ repressors and act additively with MYC2 in the activation of jasmonate responses. Plant Cell **23:** 701–715.

Figueroa, P., and Browse, J. (2012). The Arabidopsis *JAZ2* promoter contains a G-Box and thymidine-rich module that are necessary and sufficient for jasmonate-dependent activation by MYC transcription factors and repression by JAZ proteins. Plant Cell Physiol. **53:** 330–343.

Fondell, J.D. (2013). The Mediator complex in thyroid hormone receptor action. Biochim. Biophys. Acta **1830:** 3867–3875.

Fonseca, S., Chini, A., Hamberg, M., Adie, B., Porzel, A., Kramell, R., Miersch, O., Wasternack, C., and Solano, R. (2009). (+)-7-*iso*-Jasmonoyl-L-isoleucine is the endogenous bioactive jasmonate. Nat. Chem. Biol. **5:** 344–350.

Gimenez-Ibanez, S., Boter, M., and Solano, R. (2015). Novel players fine-tune plant trade-offs. Essays Biochem. **58:** 83–100.

Gonzalez, D., Bowen, A.J., Carroll, T.S., and Conlan, R.S. (2007). The transcription corepressor LEUNIG interacts with the histone deacetylase HDA19 and mediator components MED14 (SWP) and CDK8 (HEN3) to repress transcription. Mol. Cell. Biol. **27:** 5306–5315.

Grigorova, B., Mara, C., Hollender, C., Sijacic, P., Chen, X., and Liu, Z. (2011). LEUNIG and SEUSS co-repressors regulate *miR172* expression in *Arabidopsis* flowers. Development **138:** 2451–2456.

Hellens, R.P., Allan, A.C., Friel, E.N., Bolitho, K., Grafton, K., Templeton, M.D., Karunairetnam, S., Gleave, A.P., and Laing, W.A. (2005). Transient expression vectors for functional genomics, quantification of promoter activity and RNA silencing in plants. Plant Methods **1:** 13.

Hou, X., Lee, L.Y., Xia, K., Yan, Y., and Yu, H. (2010). DELLAs modulate jasmonate signaling via competitive binding to JAZs. Dev. Cell **19:** 884–894.

Howe, G.A., and Jander, G. (2008). Plant immunity to insect herbivores. Annu. Rev. Plant Biol. **59:** 41–66.

Hu, P., Zhou, W., Cheng, Z., Fan, M., Wang, L., and Xie, D. (2013). *JAV1* controls jasmonate-regulated plant defense. Mol. Cell **50:** 504–515.

Huang, J., DeBowles, D., Esfandiari, E., Dean, G., Carpita, N.C., and Haughn, G.W. (2011). The Arabidopsis transcription factor *LUH/MUM1* is required for extrusion of seed coat mucilage. Plant Physiol. **156:** 491–502.

Jennings, B.H., and Ish-Horowicz, D. (2008). The Groucho/TLE/Grg family of transcriptional co-repressors. Genome Biol. **9:** 205.

Jiang, L., et al. (2013). DWARF 53 acts as a repressor of strigolactone signalling in rice. Nature **504:** 401–405.

Kazan, K., and Manners, J.M. (2013). MYC2: The master in action. Mol. Plant **6:** 686–703.

Ke, J., Ma, H., Gu, X., Thelen, A., Brunzelle, J.S., Li, J., Xu, H.E., and Melcher, K. (2015). Structural basis for recognition of diverse transcriptional repressors by the TOPLESS family of corepressors. Sci. Adv. **1:** e1500107.

Kidd, B.N., Edgar, C.I., Kumar, K.K., Aitken, E.A., Schenk, P.M., Manners, J.M., and Kazan, K. (2009). The mediator complex subunit PFT1 is a key regulator of jasmonate-dependent defense in *Arabidopsis.* Plant Cell **21:** 2237–2252.

Kornberg, R.D. (2007). The molecular basis of eukaryotic transcription. Proc. Natl. Acad. Sci. USA **104:** 12955–12961.

Krogan, N.T., Hogan, K., and Long, J.A. (2012). APETALA2 negatively regulates multiple floral organ identity genes in *Arabidopsis* by

recruiting the co-repressor TOPLESS and the histone deacetylase HDA19. Development **139:** 4180–4190.

Lee, J.E., and Golz, J.F. (2012). Diverse roles of Groucho/Tup1 co-repressors in plant growth and development. Plant Signal. Behav. **7:** 86–92.

Lee, N., Park, J., Kim, K., and Choi, G. (2015). The transcriptional coregulator LEUNIG_HOMOLOG inhibits light-dependent seed germination in *Arabidopsis.* Plant Cell **27:** 2301–2313.

Li, L., Zhao, Y., McCaig, B.C., Wingerd, B.A., Wang, J., Whalon, M.E., Pichersky, E., and Howe, G.A. (2004). The tomato homolog of CORONATINE-INSENSITIVE1 is required for the maternal control of seed maturation, jasmonate-signaled defense responses, and glandular trichome development. Plant Cell **16:** 126–143.

Li, X., Lin, H., Zhang, W., Zou, Y., Zhang, J., Tang, X., and Zhou, J.M. (2005). Flagellin induces innate immunity in nonhost interactions that is suppressed by *Pseudomonas syringae* effectors. Proc. Natl. Acad. Sci. USA **102:** 12990–12995.

Liu, Z., and Karmarkar, V. (2008). Groucho/Tup1 family co-repressors in plant development. Trends Plant Sci. **13:** 137–144.

Liu, Z., and Meyerowitz, E.M. (1995). LEUNIG regulates *AGAMOUS* expression in Arabidopsis flowers. Development **121:** 975–991.

Long, J.A., Ohno, C., Smith, Z.R., and Meyerowitz, E.M. (2006). TOPLESS regulates apical embryonic fate in *Arabidopsis.* Science **312:** 1520–1523.

Lorenzo, O., Chico, J.M., Sánchez-Serrano, J.J., and Solano, R. (2004). *JASMONATE-INSENSITIVE1* encodes a MYC transcription factor essential to discriminate between different jasmonate-regulated defense responses in *Arabidopsis.* Plant Cell **16:** 1938–1950.

Love, M.I., Huber, W., and Anders, S. (2014). Moderated estimation of fold change and dispersion for RNA-seq data with DESeq2. Genome Biol. **15:** 550.

Malik, S., and Roeder, R.G. (2010). The metazoan Mediator co-activator complex as an integrative hub for transcriptional regulation. Nat. Rev. Genet. **11:** 761–772.

Nakagawa, T., Kurose, T., Hino, T., Tanaka, K., Kawamukai, M., Niwa, Y., Toyooka, K., Matsuoka, K., Jinbo, T., and Kimura, T. (2007). Development of series of gateway binary vectors, pGWBs, for realizing efficient construction of fusion genes for plant transformation. J. Biosci. Bioeng. **104:** 34–41.

Oh, E., Zhu, J.Y., Ryu, H., Hwang, I., and Wang, Z.Y. (2014). TOPLESS mediates brassinosteroid-induced transcriptional repression through interaction with BZR1. Nat. Commun. **5:** 4140.

Pauwels, L., et al. (2010). NINJA connects the co-repressor TOPLESS to jasmonate signalling. Nature **464:** 788–791.

Penninckx, I.A., Eggermont, K., Terras, F.R., Thomma, B.P., De Samblanx, G.W., Buchala, A., Métraux, J.P., Manners, J.M., and Broekaert, W.F. (1996). Pathogen-induced systemic activation of a plant defensin gene in *Arabidopsis* follows a salicylic acid-independent pathway. Plant Cell **8:** 2309–2323.

Pi, L., Aichinger, E., van der Graaff, E., Llavata-Peris, C.I., Weijers, D., Hennig, L., Groot, E., and Laux, T. (2015). Organizer-derived WOX5 signal maintains root columella stem cells through chromatin-mediated repression of *CDF4* expression. Dev. Cell **33:** 576–588.

Poss, Z.C., Ebmeier, C.C., and Taatjes, D.J. (2013). The Mediator complex and transcription regulation. Crit. Rev. Biochem. Mol. Biol. **48:** 575–608.

Qi, T., Song, S., Ren, Q., Wu, D., Huang, H., Chen, Y., Fan, M., Peng, W., Ren, C., and Xie, D. (2011). The Jasmonate-ZIM-domain proteins interact with the WD-Repeat/bHLH/MYB complexes to regulate Jasmonate-mediated anthocyanin accumulation and trichome initiation in *Arabidopsis thaliana.* Plant Cell **23:** 1795–1814.

Qi, T., Wang, J., Huang, H., Liu, B., Gao, H., Liu, Y., Song, S., and Xie, D. (2015). Regulation of jasmonate-induced leaf senescence by antagonism between bHLH subgroup IIIe and IIId factors in *Arabidopsis.* Plant Cell **27:** 1634–1649.

Sheard, L.B., et al. (2010). Jasmonate perception by inositol-phosphate-potentiated COI1-JAZ co-receptor. Nature **468:** 400–405.

Sitaraman, J., Bui, M., and Liu, Z. (2008). LEUNIG_HOMOLOG and LEUNIG perform partially redundant functions during Arabidopsis embryo and floral development. Plant Physiol. **147:** 672–681.

Song, S., Qi, T., Fan, M., Zhang, X., Gao, H., Huang, H., Wu, D., Guo, H., and Xie, D. (2013). The bHLH subgroup IIId factors negatively regulate jasmonate-mediated plant defense and development. PLoS Genet. **9:** e1003653.

Song, S., Huang, H., Wang, J., Liu, B., Qi, T., and Xie, D. (2017). MYC5 is involved in jasmonate-regulated plant growth, leaf senescence and defense responses. Plant Cell Physiol. **58:** 1752–1763.

Soutourina, J., Wydau, S., Ambroise, Y., Boschiero, C., and Werner, M. (2011). Direct interaction of RNA polymerase II and mediator required for transcription *in vivo.* Science **331:** 1451–1454.

Sridhar, V.V., Surendrarao, A., Gonzalez, D., Conlan, R.S., and Liu, Z. (2004). Transcriptional repression of target genes by LEUNIG and SEUSS, two interacting regulatory proteins for Arabidopsis flower development. Proc. Natl. Acad. Sci. USA **101:** 11494–11499.

Stahle, M.I., Kuehlich, J., Staron, L., von Arnim, A.G., and Golz, J.F. (2009). YABBYs and the transcriptional corepressors LEUNIG and LEUNIG_HOMOLOG maintain leaf polarity and meristem activity in *Arabidopsis.* Plant Cell **21:** 3105–3118.

Staswick, P.E., and Tiryaki, I. (2004). The oxylipin signal jasmonic acid is activated by an enzyme that conjugates it to isoleucine in *Arabidopsis.* Plant Cell **16:** 2117–2127.

Szemenyei, H., Hannon, M., and Long, J.A. (2008). TOPLESS mediates auxin-dependent transcriptional repression during Arabidopsis embryogenesis. Science **319:** 1384–1386.

Tao, Q., Guo, D., Wei, B., Zhang, F., Pang, C., Jiang, H., Zhang, J., Wei, T., Gu, H., Qu, L.J., and Qin, G. (2013). The TIE1 transcriptional repressor links TCP transcription factors with TOPLESS/TOPLESS-RELATED corepressors and modulates leaf development in *Arabidopsis.* Plant Cell **25:** 421–437.

Thines, B., Katsir, L., Melotto, M., Niu, Y., Mandaokar, A., Liu, G., Nomura, K., He, S.Y., Howe, G.A., and Browse, J. (2007). JAZ repressor proteins are targets of the SCF(COI1) complex during jasmonate signalling. Nature **448:** 661–665.

Van Wees, S.C., Van Pelt, J.A., Bakker, P.A., and Pieterse, C.M. (2013). Bioassays for assessing jasmonate-dependent defenses triggered by pathogens, herbivorous insects, or beneficial rhizobacteria. Methods Mol. Biol. **1011:** 35–49.

Walker, M., Tehseen, M., Doblin, M.S., Pettolino, F.A., Wilson, S.M., Bacic, A., and Golz, J.F. (2011). The transcriptional regulator LEUNIG_HOMOLOG regulates mucilage release from the Arabidopsis testa. Plant Physiol. **156:** 46–60.

Wang, Y., et al. (2017). GSA: genome sequence archive. Genomics Proteomics Bioinformatics **15:** 14–18.

Wang, L., Wang, S., and Li, W. (2012). RSeQC: Quality control of RNA-seq experiments. Bioinformatics **28:** 2184–2185.

Wang, L., Kim, J., and Somers, D.E. (2013). Transcriptional corepressor TOPLESS complexes with pseudoresponse regulator proteins and histone deacetylases to regulate circadian transcription. Proc. Natl. Acad. Sci. USA **110:** 761–766.

Wasternack, C., and Hause, B. (2013). Jasmonates: Biosynthesis, perception, signal transduction and action in plant stress response, growth and development. An update to the 2007 review in Annals of Botany. Ann. Bot. **111:** 1021–1058.

Xie, D.X., Feys, B.F., James, S., Nieto-Rostro, M., and Turner, J.G. (1998). *COI1*: An Arabidopsis gene required for jasmonate-regulated defense and fertility. Science **280:** 1091–1094.

Xu, L., Liu, F., Lechner, E., Genschik, P., Crosby, W.L., Ma, H., Peng, W., Huang, D., and Xie, D. (2002). The SCF(^{COI1}) ubiquitin-ligase complexes are required for jasmonate response in *Arabidopsis.* Plant Cell **14:** 1919–1935.

Yan, J., Zhang, C., Gu, M., Bai, Z., Zhang, W., Qi, T., Cheng, Z., Peng, W., Luo, H., Nan, F., Wang, Z., and Xie, D. (2009). The Arabidopsis CORONATINE INSENSITIVE1 protein is a jasmonate receptor. Plant Cell **21:** 2220–2236.

Yin, J.W., and Wang, G. (2014). The Mediator complex: A master coordinator of transcription and cell lineage development. Development **141:** 977–987.

Yoo, S.D., Cho, Y.H., and Sheen, J. (2007). Arabidopsis mesophyll protoplasts: A versatile cell system for transient gene expression analysis. Nat. Protoc. **2:** 1565–1572.

Yu, G., Wang, L.G., Han, Y., and He, Q.Y. (2012). clusterProfiler: An R package for comparing biological themes among gene clusters. OMICS **16:** 284–287.

Zhai, Q., Yan, L., Tan, D., Chen, R., Sun, J., Gao, L., Dong, M.Q., Wang, Y., and Li, C. (2013). Phosphorylation-coupled proteolysis of the transcription factor MYC2 is important for jasmonate-signaled plant immunity. PLoS Genet. **9:** e1003422.

Zhai, Q., Li, L., An, C., and Li, C. (2017a). Conserved function of Mediator in regulating nuclear hormone receptor activation between plants and animals. Plant Signal. Behav.**13:** 1403709.

Zhai, Q., Yan, C., Li, L., Xie, D., and Li, C. (2017b). Jasmonates. In Hormone Metabolism and Signaling in Plants, Smith, S.M., Li, C., and Li, J., eds. (London: Elsevier), pp. 243–272.

Zhang, F., et al. (2015). Structural basis of JAZ repression of MYC transcription factors in jasmonate signalling. Nature **525:** 269–273.

Zhang, F., Ke, J., Zhang, L., Chen, R., Sugimoto, K., Howe, G.A., Xu, H.E., Zhou, M., He, S.Y., and Melcher, K. (2017). Structural insights into alternative splicing-mediated desensitization of jasmonate signaling. Proc. Natl. Acad. Sci. USA **114:** 1720–1725.

Zhu, Z., An, F., Feng, Y., Li, P., Xue, L., A, M., Jiang, Z., Kim, J.M., To, T.K., Li, W., Zhang, X., and Yu, Q., et al. (2011). Derepression of ethylene-stabilized transcription factors (EIN3/EIL1) mediates jasmonate and ethylene signaling synergy in *Arabidopsis.* Proc. Natl. Acad. Sci. USA **108:** 12539–12544.